Transition from subduction to arc-continent collision: Geologic and neotectonic evolution of Savu Island, Indonesia

Ron Harris
Michael W. Vorkink
Department of Geological Sciences, Brigham Young University, Provo, Utah 84602, USA

Carolus Prasetyadi
Fakultas Teknologi Mineral, Universitas Pembangunan Nasional, Yogyakarta, Indonesia

Elizabeth Zobell
Nova Roosmawati
Department of Geological Sciences, Brigham Young University, Provo, Utah 84602, USA

Marjorie Apthorpe
Apthorpe Palaeontology Pty Ltd, 69 Bacchante Circle, Ocean Reef, Western Australia 6027, Australia

ABSTRACT

Field analyses of stratigraphy, structure, and tectonic geomorphology of Savu Island define the age and provenance of accreted Australian continental margin sequences and overlying synorogenic cover, and the structure, kinematics, and uplift history of the transition from subduction to collision in the eastern Sunda-Banda arc. The results highlight the dominant influence of lower plate composition and structure in shaping Savu Island and initiating intraforearc shortening. Provenance and biostratigraphic analyses of rocks accreted to the edge of the Sunda-Banda forearc indicate that they mostly consist of Triassic to Cretaceous synrift and postrift successions of the Australian continental margin. These rocks are similar in composition and provenance to Gondwana sequence units found throughout the Banda arc to the east, such as the Triassic Babulu, Jurassic Wai Luli, and Cretaceous Nakfunu Formations of Timor. Previously unrecognized units of pillow basalt are found interlayered with Jurassic beds and incorporated into mélange and mud diapirs. These basalt occurrences have major and trace element compositions similar to those of Indian Ocean mid-oceanic ridge basalt and are likely associated with Jurassic development of the Scott Plateau volcanic margin. South-directed thrusting of these units via a duplex thrust system detached the Middle Triassic section of the underthrust Scott Plateau.

The Savu thrust system consists of a series of active north-directed thrust faults found onshore and offshore the north coast of Savu. Thrust faults mapped onshore, penetrated by the Savu #1 well and imaged in vintage seismic reflection profiles, offset the youngest deposits of Savu. The uplift history and deformation pattern associated with the Savu thrust is investigated at a variety of temporal scales. Foraminifera-rich synorogenic deposits indicate low average surface uplift rates until after 1.9 Ma ago, when pelagic chalk deposits were raised from depths of >2500 m to the surface in fewer than 1 Ma. Island emergence is well documented by uplifted coral terraces that encrust the highest ridges to 338 m elevation. U/Th analysis of uplifted coral yields ages of 122 ka near sea level, indicating slow uplift rates of 0.2 mm/a over the past 400 ka.

Most synorogenic deposits are stripped from the south coast, exposing parts of the accretionary wedge. The deeply eroded nature of this part of the island, combined with its steep first-order stream gradients, indicates that it underwent rapid rock uplift and exhumation in the past 1–2 Ma. However, the south coast region is now subsiding, as evidenced by drowned streams and south-tilted, submerging coral terraces. Streams draining north over the Savu thrust system show convex-upward patterns with gradients commonly associated with intermediate uplift rates. Flights of coral terraces also document growth of the island to the north above thrust-related folds.

These results inform us that the transition from subduction to collision involves (1) strain partitioning away from the subduction zone into the upper plate, (2) forearc closure, (3) structure inherited from the lower plate, (4) initiation of a crustal suture zone, and (5) uplift and exhumation of the accretionary wedge.

INTRODUCTION

Rarely is the critical transition from subduction to collision preserved in advanced orogens or exposed in active ones. This transition is important because it records the inception of mountain building, which includes (1) underthrusting, shortening, and accretion of passive continental margin units, (2) emplacement of ophiolites, (3) initiation of synorogenic sedimentation, (4) development of continental foredeeps, (5) creation of orogenic topography, and (6) initiation of subduction polarity reversal (Harris, 2004). The active Sunda-Banda arc-continent collision zone of Australasia (Fig. 1) is used as a modern analog for each of these inaugural collisional processes (see Animation 1). However, what happens to the Sunda-Banda arc-trench system, as it is underthrust by the Australian continental margin, remains widely contested due to few data (i.e., Carter et al., 1976; Chamalaun and Grady, 1978; Hamilton, 1979; Bowin et al., 1980; Harris, 1991, 2006; Charlton, 1991; Kaneko et al., 2007).

One of the least understood parts of the Banda orogen is the transition from subduction to collision in the region around Savu Island (Audley-Charles, 1985; Chamalaun et al.,

1982; McCaffrey, 1988). This region occupies the Sunda-Banda arc transition, which extends between the eastern Sunda arc island of Flores and western Banda arc island of Wetar (Fig. 1). Although marine geophysical studies have been conducted in the Savu region (Bowin et al., 1980; Silver et al., 1983; Breen et al., 1986; Karig et al., 1987; Masson et al., 1991; van der Werff, 1995a, 1995b), the fundamental geological and structural makeup is poorly delimited due to lack of detailed field observations and age determinations. These determinations are needed before structural reconstructions of this region are possible. Savu also provides a way to investigate other key aspects of arc-continent collision processes, such as structural style (mélange versus fold-thrust), surface uplift patterns and rates, timing of deformation (collision propagation rate), and geological hazards (active faults).

To address these questions we conducted a detailed field investigation including geological mapping of the island at a scale of 1:25,000. During the mapping we analyzed the composi-

tion and structure of each geological unit, which includes biostratigraphic relations, sandstone provenance, U/Pb age of detrital zircon, basalt geochemistry, depth versus age analysis of foraminifera in synorogenic units, analysis of well data and offshore seismic lines, and tectonic geomorphology of uplifted coral terraces and stream profiles. The overall objective is to document the tectonic evolution of Savu, which represents the initial, formative stages of arc-continent collision and suture development.

TRANSITION FROM SUBDUCTION TO COLLISION IN THE SAVU REGION

Savu Island provides the earliest glimpse of mountain building from accretion of Australian continental margin cover units to the Sunda-Banda arc, and the initiation of collision-related strain partitioning away from the Java trench. The accretionary system formed initially from middle Miocene to Pliocene subduction of Jurassic and Cretaceous oceanic lithosphere at the Sunda-Banda trench (Fig. 2). During the

latest Pliocene the Scott Plateau of the Australian continental margin entered the trench, which increased dramatically its accretionary influx and transformed it into a continental foredeep and incipient foreland fold-and-thrust belt (Animation 1).

The characteristics of the accretionary wedge south of Savu differ from what is found on either side. To the west is the 6-km-deep Java Trench, tectonically underlain by Jurassic oceanic crust, and to the east is the 2–3-km-deep Timor Trough, tectonically underlain by continental crust. Where the Java Trench ends is a diffuse zone of deformation that takes on the characteristics of a foreland fold and thrust belt (Audley-Charles, 1986a, 2004) with a deformation front of mud ridges (Breen et al., 1986; Masson et al., 1991). Seismic images of the deformation front south of Savu (Breen et al., 1986; Karig et al., 1987) show the décollement at a stratigraphic level of highly overpressured Jurassic mudstone that is the major source for mud diapirs and mélange matrix in Timor (Harris et al., 1998). The deformation front also protrudes to
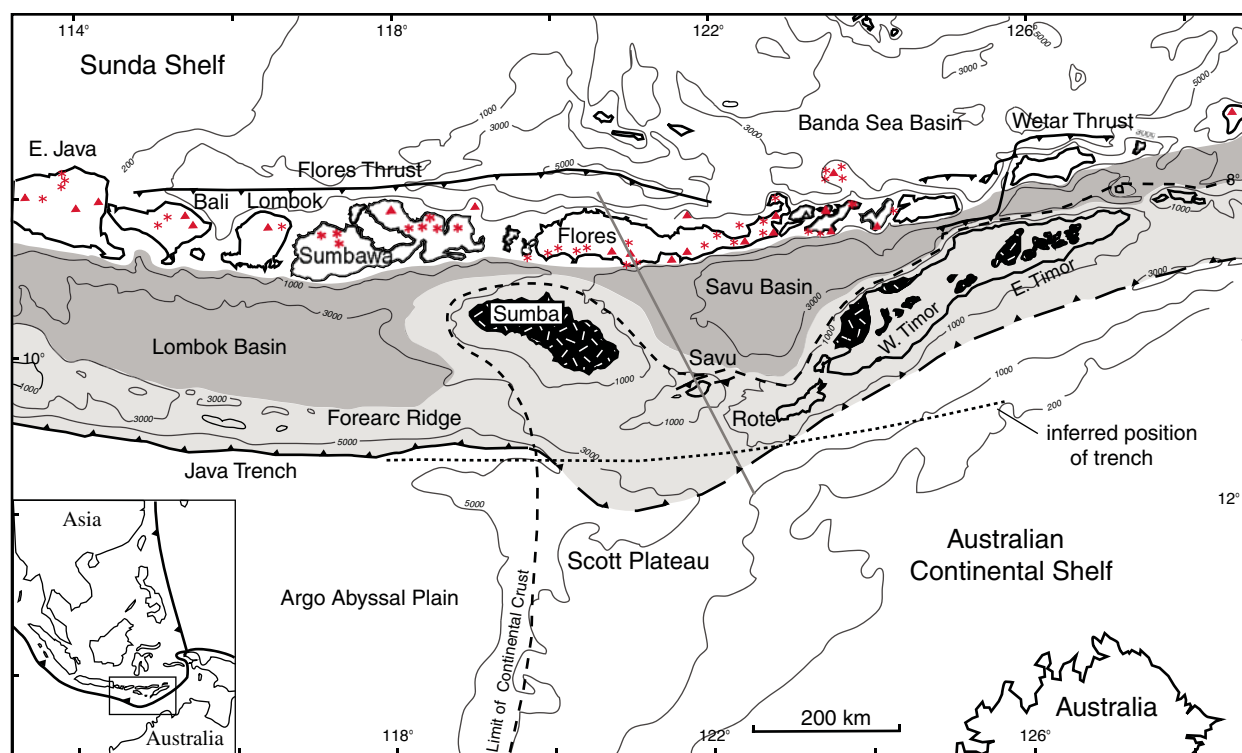
Figure 1. Map of major tectonic features and domains of the active Sunda-Banda arc-continent collision. Dark gray is forearc basin and light gray is uplifted forearc basement and accretionary wedge. Black with white stippled pattern is exposed forearc basement or Banda terrane (Harris, 1992). Dashed line estimates the position of underthrust Australian continental crust and the Scott Plateau prong. The Sumba Ridge is in the same position as the dashed line west of Sumba and immediately north of Savu. Dark lines with teeth are active thrust faults with teeth on hanging wall. Red triangles are active volcanoes; stars are late Quaternary volcanoes. North-northwest–south-southeast line is cross section in Figure 2. Dotted line is inferred position of the precollisional Sunda-Banda trench, which is now underlain by continental crust and is the Timor Trough.

the south to 100 km beyond its position south of Sumba and Timor (Fig. 1). Associated with this is a change in the accretionary slope angle to only a few degrees compared to 5°–6° to the west and east (Harris, 1991).

These features are interpreted as a response to underthrusting of the Scott Plateau and southward propagation of the basal décollement into its weak sedimentary cover units. The change in accretionary slope taper angle is interpreted as response to a dramatic reduction in basal traction from oceanic crust to mudstone (Harris, 1991). The reduction in slope angle is accommodated by a series of top-down-to-the-south halfgrabens that form south of Savu (van der Werff, 1995a), indicating a phase of wedge collapse.

Underthrusting of the Scott Plateau

The emergence of the Sunda-Banda forearc on the islands of Sumba and Savu is one of the most vivid physiographic expressions of the transition from subduction to collision. The precollisional accretionary ridge (Lombok Ridge) to the west of Sumba is at a water depth of ~3–4 km. East of Sumba the accretionary ridge rises to form an east-northeast–west-southwest bathymetric high near sea level marked by the islands of Dana, Rai Jua, and Savu. These differences in elevation between precollisional and transitional settings can be attributed to uplift of

the accretionary wedge by underthrusting and shortening of the Scott Plateau. Underthrusting alone can account for at least 2–3 km of uplift, which is the difference in bathymetry between the Scott Plateau and surrounding oceanic crust.

The structure and orientation of the Scott Plateau cause major lateral discontinuities in the Banda orogen. The Scott Plateau formed during Late Jurassic rifting and has an estimated crustal thickness of 17–18 km (Symonds et al., 1998). Adjacent magnetic lineations and its rift basins show that the Scott Plateau was stretched to the northwest at the same time as it was juxtaposed against oceanic crust along transform faults on its northeast and southwest sides. The transform-faulted northeast side underthrusts the Sunda-Banda forearc. This collisional geometry means that the northeast-southwest–oriented rift basins of the Scott Plateau are colliding with the forearc subparallel to their axes, versus perpendicular to their axes, as most reconstructions of arc-continent collision assume. For example, the east-northeast–west-southwest Savu Ridge rises where the axis of the Scott Trough, which is the largest rift basin of the Scott Plateau, underthrusts the Sunda-Banda forearc.

The northwest-trending protrusion of the Scott Plateau would have first collided with the east-west Java Trench south of Sumba, causing the collision to propagate along the northeast edge of the plateau toward Savu. Although the uplift history

of Sumba is well defined (Chamalaun et al., 1982; Pirazzoli et al., 1993), there are no data available from the Savu region to test this hypothesis, which is a major focus of our investigation.

Farther to the east the accretionary wedge in Timor rises to 2000–3000 m in elevation. It also exposes collision-related metamorphic rocks exhumed on the north coast of Timor from depths as great as 30 km (Berry and Grady, 1981). These differences in structural and topographic elevation between Timor and Savu are attributed to differences in the thickness of the Australian continental crust that has underthrust these regions, and greater amounts of shortening (Harris, 1991). The Australian continental slope that has underthrust Timor is as much as 3000 m above the Scott Plateau (Fig. 1), and is in a more advanced stage of collision. Several lines of evidence (Audley-Charles, 1986b) support the fact that the east-northeast–west-southwest continental slope east of the Scott Plateau first collided with the Banda arc in the East Timor region and has propagated westward from Timor to Savu at a rate of ~110 km/Ma (Harris, 1991). The V-shaped nature of the northwest Australian continental margin between Sumba and Timor predicts that the Savu region, which occupies the point of the V, may represent the youngest part of the Banda arc-continent collision, a collisional stage that was happening south of Sumba and in Timor 2–5 Ma ago.

Animation 1. Sand box experiment movie illustrating various phases of the arc-continent collision observed throughout the Banda Arc. You will need Windows Media Player or a multimedia player such as Quicktime Media Player to view this file. If you are viewing the PDF of this paper or reading it offline, please visit http://dx.doi .org/10.1130/GES00209.S1 or the full-text article at http://geosphere.gsapubs.org to view the animation.

The model is designed to test the influence of inserting a flat-flexible backstop (forearc basement) into the accretionary wedge as observed in Savu and older parts of the

Banda Orogen exposed in Timor. A stratigraphy of lime and sand is scaled to thicknesses observed for cover sequences of the Scott Plateau, while plasticine clay is used to represent rigid forearc basement.

The rheological properties of these materials are well documented (i.e., Huiqi et al., 1992) and provide reasonable approximations of contrasts in mechanical strength found between Australian cover rocks and forearc basement. The model is scaled at a ratio of 1 cm = 1 km. A 1 cm layer of plasticine clay extends on top of a 3.7-cm thick section of alternating white lime and red lime/sand layers (Gondwana Sequence lower cover units of Australian continental margin). In front of the plasticine is a 1.2-cm thick section of alternating units (Australian Passive Margin Sequence of the upper cover of the Australian continental margin). Shear strengths are 161 and 176 (Pa) for the lime and sand/lime layers, respectively.

The experiment and others like it produce an upper structural level of trench-ward verging imbricate thrust sheets of only the upper sections of the cover in front and above the backstop. The lower section of cover forms a

duplex system of large isoclinal, recumbent folds, and out of syncline thrusts. Initially the upper thrust sheets and faults dip between 20°–30°, but with accretion of new thrust sheets to the front of the stack, older sheets are tilted progressively more arcward until they become near vertical and even slightly overturned.

Maximum uplift occurs in the imbricate fan above the leading edge of the backstop. This part of the accretionary wedge would be the first to emerge above sea level and stripped by erosion, as observed in Savu. The backstop is also uplifted and folded into a concave down geometry. A highly attenuated mélange-like zone develops immediately beneath the plasticine forearc nappe due to very high shear strain.

Insertion of the flat flexible backstop into the layered section produces two distinct structural domains: frontal accretion above and duplexing beneath the backstop. The same patterns of accretion and backstop deformation are found throughout the Banda arc-continent collision (Harris, 1991). Only the early stages of the model are like the Savu phase of collision. Later stages are more emblematic of the Timor region.
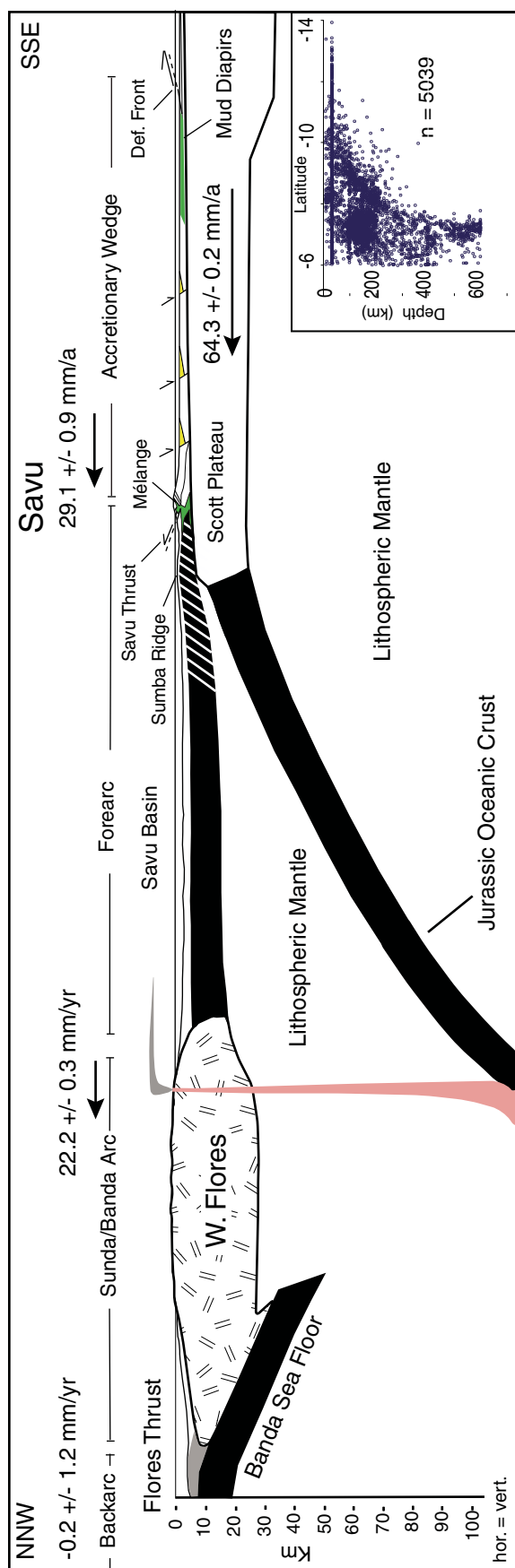
Figure 2. Crustal cross section through the transition from subduction to collision (see Fig. 1 for line of section). Global positioning system velocities are relative to the Sunda Shelf (backarc) in the direction of shortening (Nugroho et al., 2009). White—continental crust, black—oceanic crust, striped—Banda terrane, green—mélange, yellow—extensional basins from wedge collapse. Blue dots are earthquake hypocenters outlining subducting slab.

North of Savu the accretionary wedge abuts against the Sumba Ridge via the north-directed Savu thrust (Reed et al., 1986). The Sumba Ridge extends southeast from Sumba to Savu and northeast from Savu to Timor. The eastern arm of the V is uplifted and exposed throughout Timor as a series of high-level crystalline nappes with Asian affinity sedimentary and igneous cover (e.g., Molengraaff, 1912; Brouwer, 1925). The tectonic significance of these rocks, and their association with the Sunda-Banda forearc and Sumba, was recognized by Audley-Charles (1985) and Carter et al. (1976). We interpret the Sumba Ridge as the forearc crustal outline of the northern V-shaped edge of the underthrust Australian continental margin. Where the continental margin is thin, such as the Scott Plateau (Fig. 2), the amount of uplift is much less. This interpretation differs from previous models that represent the low-density rocks underlying Sumba as a continental fragment trapped in the upper plate (Hamilton, 1979; Chamalaun et al., 1982). Other models have considered the possibility that Sumba represents an anomalously thick part of forearc basement (i.e., Rutherford et al., 2001). However, none of these interpretations relate the uplifted forearc rocks exposed in Sumba to underthrusting of the continental Scott Plateau.

In summary, the tectonic features associated with underthrusting of the Scott Plateau and the transition from subduction to collision in the Savu region include: (1) initiation of northward-verging thrust systems (Flores and Savu thrusts), (2) migration of shallow seismicity (<50 km) away from the trench into the forearc and backarc, (3) uplift of the forearc basin (Sumba) and ridge (Savu), (4) abrupt widening of the accretionary wedge by >100 km, (5) accretionary wedge collapse (surface slope angle reduction from 5° at Lombok Ridge to 2° south of Savu), (6) formation of slope basins, and (7) extensive mud diapirism. Features 1–3 we relate to increased coupling due to positive buoyancy of the underthrust continental plate. Features 4–7 we interpret as a consequence of adjustments made by the accretionary wedge as a result of collision initiation. Some of these include basal décollement weakening as Australian continental slope units enter the trench (Harris et al., 1998).

Global Positioning System Measurements and the Distribution of Strain

High-resolution global positioning system (GPS) measurements reveal the distribution of strain throughout the transition from subduction to collision (Genrich et al., 1996; Nugroho et al., 2009). These measurements show that relative to the Sunda Shelf the motion of the Sunda-Banda

arc is increasingly coupled with the Australian plate eastward along orogenic strike (Fig. 1). GPS stations within the Asian plate show little to no motion with respect to one another and the rest of Southeast Asia, except for arc islands immediately west of Sumba, which move from 14 to 17 ± 1 mm/a in the same direction as the Australian plate relative to stable Asia. North of Sumba and Savu the motion of the Sunda-Banda arc increases to 23–25 ± 1–2 mm/a, and the inactive Sunda-Banda arc islands north of Timor move as much as 44 mm/a in the same direction as the Australian plate (Nugroho et al., 2009).

Outer arc islands of the accretionary wedge show a similar trend. Sumba, Savu, Rote, and Timor all move parallel to the Australian plate at increasing rates to the east that are slightly higher than motions of adjacent parts of the Sunda-Banda arc. Where subduction is dominant south of Java and Bali, most convergence is taken up at the trench. Increased coupling between the upper and lower plates in the oblique collision activates deformation throughout the arc-trench system where the buoyant Scott Plateau is underthrust near Sumba and Savu, and the Australian continental slope is underthrust beneath Timor. Timor and the adjacent volcanic islands to the north move as much as 47 ± 1 mm/a relative to the Asian plate in the same direction as Australia, which is two-thirds of the rate of the Australian plate (Nugroho et al., 2009).

Baselines measured in the direction of structural transport (north-northwest–south-southeast) from stable Australia across the Savu portion of the accretionary wedge, western Flores, and the backarc, document where most of the collisional strain is distributed during the initiation of collision. Although the majority of motion is still taken up near the deformation front, at least 7 ± 1 mm/a of convergence is measured between the north coast of Savu and western Flores, and another 22 mm/a between Flores and the Sunda Shelf (Nugroho et al., 2009). We infer that most of this convergence is localized along the Savu and Flores thrust systems (Fig. 2), with the Savu thrust only accounting for approximately one-third of the motion on the Flores thrust. Deformation associated with the Flores thrust system is well documented (Silver et al., 1983). Estimates from seismic profiles indicate from 30 to 60 km of horizontal motion of western Flores relative to the backarc. In eastern Flores little if any deformation occurs along this thrust system. If we divide the total amount of shortening estimated along the Flores thrust by the present rate of shortening measured across it (22 mm/a), it formed ca. 1.4–2.7 Ma ago. This is most likely a minimum estimate, because there is evidence that rates increase as the thrust propagates.

GEOLOGY OF SAVU

From field mapping (Fig. 3) and petrographic, biostratigraphic, radiometric, and geochemical sample analysis, we identify four lithotectonic units in Savu (Figs. 3 and 4). They include precollisional continental margin cover sequences of the Scott Plateau that accreted to the edge of the Asian plate, which are overlain by synorogenic deposits. Scott Plateau continental margin cover sequences include Triassic and Jurassic siliciclastic rocks that are similar to the Babulu and Wai Luli Formations of the prerift Gondwana sequence (Harris et al., 2000), and the postrift Australian passive margin sequence (Haig et al., 2007), which includes rocks similar to the Nakfunu Formation of Timor (Figs. 4 and 5). Mélange with blocks from most of these units and others not found in outcrop (Fig. 5G) surround a thrust-faulted package of Gondwana sequence units (Fig. 3). All of these lithologies are repeated by east-northeast–west-southwest–trending thrust sheets directed north-northwest and south-southeast (Fig. 3). Unconformably overlying synorogenic units (Figs. 5A and 5H) include foraminifera-rich deep-water chalk and uplifted coral terraces, which provide useful data for reconstructing the islands uplift history.

Babulu Formation

The Late Triassic Babulu Formation in West Timor was first described by Gianni (1971), and consists mostly of interbedded sandstone and shale. Approximately 250 m of Babulu-like successions are repeatedly exposed in thrust sheets near the southern coast in central Savu (Figs. 5A, 5B). Most of the section consists of thinly bedded limestone with chert nodules, shale, siltstone, and thick sandstone beds. A marker bed in the middle part of the section consists of a 10-cm-thick packstone containing *Halobia* sp., which is a well-documented index fossil for the Carnian–Norian (Gianni, 1971; Bird and Cook, 1991).

The limestone section of the Babulu Formation in Savu is sandwiched between two massive to bedded sandstone units. The basal unit is a bedded, olive to tan, micaceous, moderately to poorly sorted sandstone with iron concretion layers (Fig. 5A). The upper massive unit is red, coarse-grained sandstone named here the Pedaro sandstone after Pedaro village in central Savu (Fig. 5B).

The Pedaro Member also has concretions ranging from 5 cm to 1 m in diameter that are often stained red to black. At several locations bedding-plane surfaces of the Pedaro sandstone have large, 10–20-cm-wide, 5-cm-high mullion structures produced by bedding-plane slip. Due to its excellent exposure and unique characteristics, the Pedaro sandstone is an important stratigraphic marker unit on Savu.

Zobell (2007) investigated the provenance of sandstone units within the Babulu Formation of Savu and Timor by petrographic studies and U/Pb age analysis of detrital zircon grains. Babulu Formation sandstone is texturally immature, with large framework grains that are subangular to subrounded and plot as quartz wackes to lithic wackes on the classification diagram of Williams et al. (1982). Sandstone provenance classifications (Dickinson et al., 1983) indicate a recycled orogen provenance. All samples have significant amounts of fresh twinned feldspar, mica, and lithic fragments, indicating that the sandstone beds of the Babulu Formation were deposited close to their source region (Zobell, 2007).

U/Pb age determinations of detrital zircon grains yield major peaks at 301 Ma and 1882 Ma ago (Zobell, 2007). The youngest grain analyzed is 234.6 ± 4 Ma old and the oldest grains are Archean, with a maximum age of 2725.3 ± 37.6 Ma old. The most likely source region that satisfies all of the criteria observed is Argoland, which rifted from the Australian continent during Jurassic breakup of Gondwana. Deposition of the Babulu Formation most likely occurred in proximal nearshore to shelf break (Sawyer et al., 1993) through turbidity currents from prograding deltas (Bird and Cook, 1991).

Wai Luli Formation

The Wai Luli Formation in East Timor was first described by Audley-Charles (1968), from exposures in the Wai Luli River valley of East Timor. Similar units are also found in Savu, and consist of a basal pink calcilutite overlain by a series of pillow basalt and thick successions of massive gray mudstone with minor silt and sandstone beds (Figs. 5C, 5D).

The upper boundary of the pink calcilutite layer is marked by a discontinuous string of pillow basalt outcrops as much as tens of meters in diameter. The consistent stratigraphic position of this unit and the lateral continuity of calcilutite sections around it indicate only minor internal deformation. We interpret the pillow basalt unit as a product of Late Jurassic rift-related magmatism along the northwest Australian margin (see following discussion of basalt). The Scott Plateau is a well-known igneous province (Crawford and von Rad, 1994). Similar basalt units are also found in the Banli #1 well on the south coast of West Timor, which drilled through a section similar to that found in Savu (Sani et al., 1995).

Stratigraphically overlying the basalt unit is ~200 m of varicolored mudstone. The best

exposures of this facies are found in south-central Savu (Fig. 5D). Popcorn textures on weathered surfaces indicate the abundance of expandable clay. Thin siltstone interbeds outline recumbent, isoclinal folds throughout this facies that complicate estimates of its original thickness.

One sample from the mudstone facies yields 25 different species of spores and pollen, most of which are long ranging in time. The only short time range species is the dinoflagellate *Rigaudella aemula*. This series of dinoflagellates belongs to a genus similar to *Polystephanophorus* or *Systematophoraore*, which was originally described in southwest Germany by Klement (1960) to range into the Late Jurassic. The species brackets the age of the sample from Oxfordian to Kimmeridgian. This age is younger than samples from the Wai Luli Formation analyzed in West Timor, which yield a consistent Hettangian–Callovian age (Sawyer et al., 1993). In this regard, it is important to note that rifting migrated from northeast to southwest along the northwest Australian continental margin, consistent with younger ages for rift-related features of the Scott Plateau (Symonds et al., 1998).

Basalt

Basalt units of Savu are found in two distinctive associations. In the northern part of the island, basalt is exposed in a sheet >2 km^2 in areal extent and is surrounded by mélange. Within the mélange basalt occurs as oblate-shaped blocks 1–2 m in diameter. In the southern part of Savu, basalt layers are found as laterally continuous 10–30-m-thick interbeds of the Wai Luli Formation (Fig. 5C), and as blocks as much as 1 m in diameter near active mud volcanoes.
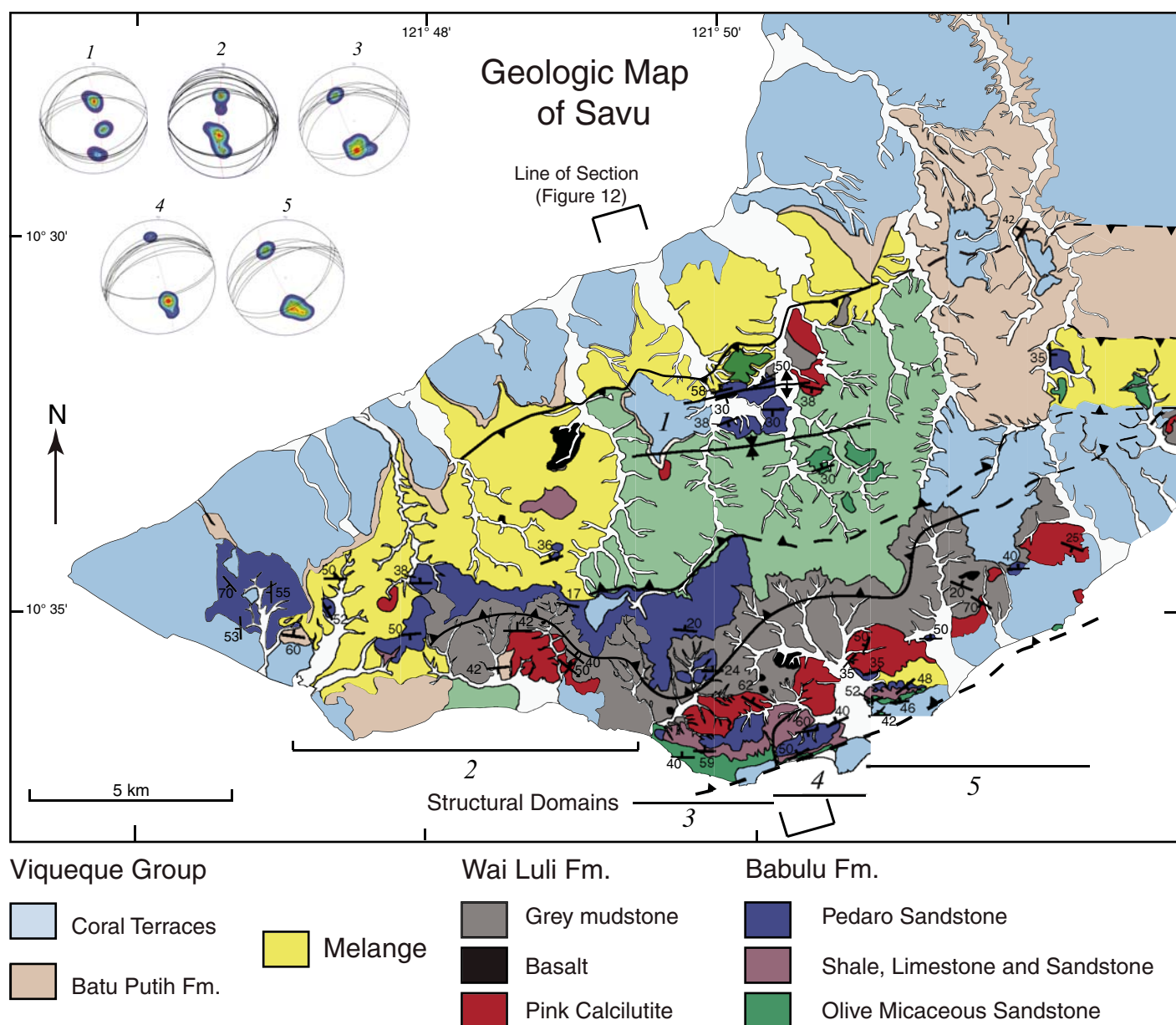

Figure 3. Geologic map of south-central Savu. Unit descriptions are given in Figure 4 and text. Light green is lower Babulu colluvium. Lower hemisphere stereographs of bedding-plane attitudes are given for each of five structural domains. The general transport direction from fold-normal lines and asymmetry is 345° ± 15°.

Whole-rock geochemical analyses of these basalt occurrences were conducted using X-ray fluorescence (Siemens SRS 303) in order to test for differences in composition and tectonic affinity. All samples are tholeiitic ferrobasalt with very similar abundances of major and trace elements (Table 1), and plot in the mid-oceanic ridge basalt (MORB) field near the boundary with ocean island basalt (OIB) (Shervais, 1982) or near the border of the MORB and within-plate basalt (WPB) fields (Figs. 6A, 6B). There is very little compositional difference in Zr/Nb versus Zr/Y between Savu basalt and Indian Ocean MORB (Fig. 6C), which plots between basalt from the Argo abyssal plain and Scott Plateau (Crawford and von Rad, 1994). Basalt found in Permian and Triassic Gondwana sequence units in Timor (Berry and Jenner, 1982) overlap other rift-related basaltic fields, but not the much more iron-rich Savu basalt. There is no overlap between Savu basalt and basalt of the Sunda-Banda forearc (Harris, 1992).

Basalt of Jurassic age forms a large welt that covers an area of 25,000 km^2 of Scott Plateau (Ramsay and Exon, 1994). The source of the basalt is interpreted as decompressional melting of the mantle during final breakup and the onset of seafloor spreading (Crawford and von Rad, 1994). The only samples from the Scott Plateau available for study thus far are from dredge halls and drill core. However, Savu provides several large exposures of the stratigraphy and morphology of these deposits, which most likely represent submarine flows that poured out over a developing rift zone along the edge of the Scott Plateau during Callovian–Oxfordian time.
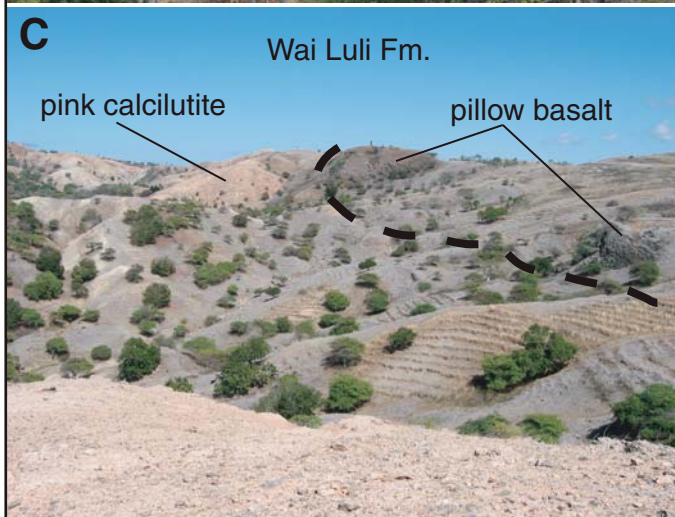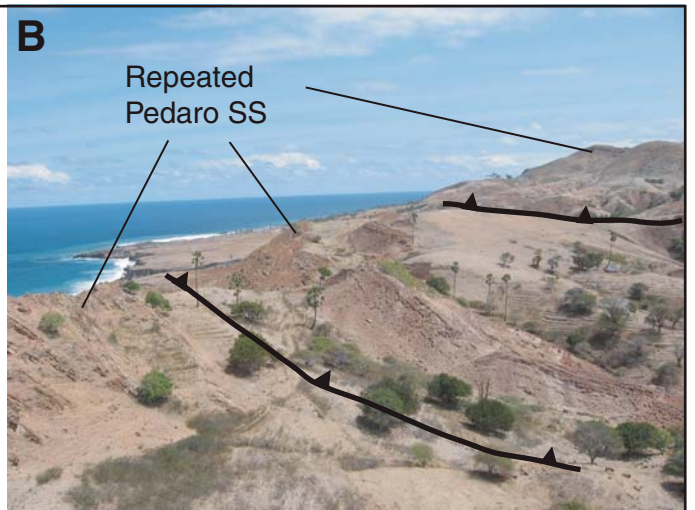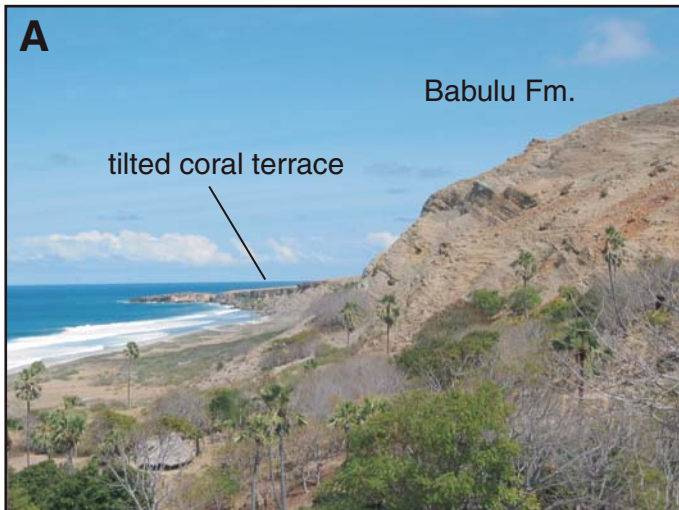
Nakfunu Formation

Small outcrops of thinly bedded red shale and ribbon chert are similar to the Early Cretaceous Nakfunu Formation of Timor (Fig. 5E). Although no fossils were found to confirm its age, the lithostratigraphic nature of the chert-rich beds is not documented from any part of the Australian continental margin sequences (Sawyer et al., 1993). However, some chert-rich rocks are found in cover sediments of the Asian affinity Banda terrane (Haile et al., 1979). We favor a Nakfunu Formation correlation due to the clear association of the chert-rich beds with other Australian affinity units. The Nakfunu Formation in Timor is commonly associated with accreted rise and slope deposits of the Australian continental margin best exposed in the Kolbano region of West Timor, and are known as the Australian passive margin sequence (Haig et al., 2007). However, in most parts of Timor where the Nakfunu Formation is exposed, it is overlain by thick deposits of Cretaceous–Miocene carbonate and shale (Sawyer et al., 1993). None of these other parts of the Australian passive margin sequence is
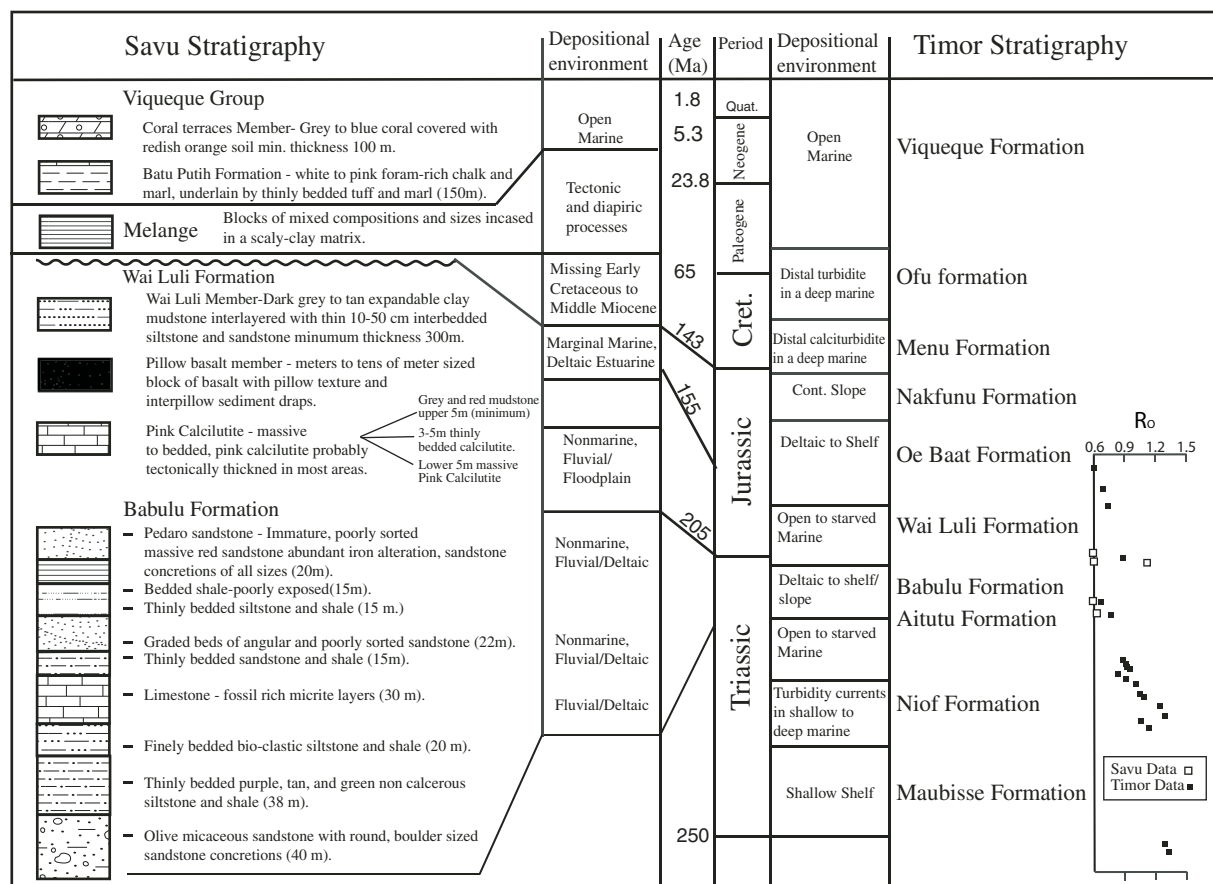
Figure 4. Permian to present stratigraphy of Savu compared with that of Timor. Most of the Australian continental units found on Savu are correlative with the Babulu, Wai Luli, and Viqueque Formations of Timor. Palynomorph data from the Wai Luli Formation on Savu indicate an age of Kimmeridgian–Oxfordian. Depositional environments are defined by comparing the abundance of kerogen type and wood content. Vitrinite reflectance (Ro) data from Timor (Harris et al., 2000) with Savu measurements show little to no thermal effects from the collision. Increasing Ro with depth most likely reflects precollisional depth of burial on the Scott Plateau (see text).

A — tilted coral terrace; Babulu Fm.

B — Repeated Pedaro SS

C — Wai Luli Fm.; pink calcilutite; pillow basalt

D

E

F

G

H — Erosional Terrace; Stage 5e Terrace?

recognized in Savu. We offer two possibilities to explain this stratigraphic anomaly. (1) Exposures of the Australian passive margin sequence are rare throughout the Banda orogen due to the fact that only the hinterland parts of the orogen are exposed, and most of the high structural level rocks are eroded away. This may be why only the lowest part of the Australian passive margin is exposed in Savu. (2) Another possibility is that much of the Australian passive margin sequence was removed from the Scott Plateau by marine currents, which are very strong through this narrow ocean gateway (Reed et al., 1986). Seismic lines across the Scott Plateau show little to no cover rocks deposited above the Gondwana sequence (Symonds et al., 1998). Dredge hauls also find only Miocene chalk directly overlying Triassic and Jurassic deposits (Crawford and von Rad, 1994).

Sumba Ridge

One of the most important contributions of seismic reflection studies in the Savu region is the imaging of the Sumba Ridge (Silver et al., 1983), which represents the southern part of the Sunda-Banda forearc. The Sumba Ridge rises

from a depth of >7 km below the sea surface in the northern Savu Basin to 1.4 km below the sea surface east of the north coast of Savu (Reed et al., 1986). Likewise, the acoustic basement of the Lombok forearc to the west, where oceanic lithosphere is subducting, is ~5 km below the sea surface (van Weering et al., 1989). We interpret these differences in structural level of forearc basement in part due to buoyancy differences between underthrust oceanic and thinned continental lithosphere (Fig. 2). The Scott Plateau is 2.5 km shallower than the adjacent ocean basin, and where both enter into the Java trench the deformation front is lifted from 6 km to 3.5 km depth, or by 2.5 km. However, to lift the forearc basement to 1.4 km, as it is found on the north coast of Savu, an additional 1.1 km of uplift is needed. The structure of Savu indicates that crustal thickening by thrusting and folding may make up the difference. In other words, underthrusting and shortening of the Scott Plateau has lifted the southern edge of the Sunda-Banda forearc basement from a precollisional depth of ~4.5 km to 1.4 km below the sea surface.

The Sumba Ridge is well exposed on Timor Island and forms deeply eroded peaks up to 2500 m above sea level. Beneath these forearc

TABLE 1. SAVU BASALT GEOCHEMISTRY

Wt%	Sv-30	Sv-56	Sv-83	Sv-4
SiO_2	48.0	46.5	47.7	49.4
TiO_2	2.6	2.7	2.0	1.7
Al_2O_3	12.8	15.5	13.1	11.2
Fe_2O_3	16.9	16.6	14.9	15.2
MnO	0.3	0.3	0.2	0.6
MgO	6.0	6.0	7.3	8.3
CaO	6.1	2.7	8.7	4.0
Na_2O	3.2	4.9	3.2	2.4
K_2O	1.8	0.7	0.2	0.0
P_2O_5	0.2	0.2	0.2	0.2
Total	97.8	96.0	97.4	93.1
ppm				
Cl	0	265	0	0
Sc	47	62	46	43
V	545	556	443	329
Cr	74	178	163	111
Ni	76	103	88	77
Cu	260	305	246	157
Zn	127	142	107	92
Ga	18	21	18	17
Rb	35	12	2	0
Sr	308	219	268	168
Y	43	36	37	30
Zr	167	172	122	133
Nb	9	8	6	9
Ba	189	32	77	3
Ce	27	18	20	16

Figure 5. Photographs of units and structural features of Savu. (A) Looking west along the south coast of Savu at resistant outcrops of Babulu Formation sandstone and shale. Note southward-tilted single coral terrace unconformably overlying exhumed Triassic units. (B) Looking west at thrust repetition of the Pedaro Member of the Babulu Formation (resistant successions). (C) String of pillow basalt layers interbedded with pink calcilutite of the Wai Luli Formation. (D) Interlayered pink and white mudstone and iron-rich sandstone. Unit is isoclinally folded, with boudinage of resistant sandstone beds. (E) Looking west at dark red-bedded chert most likely of the Cretaceous Kolbano Formation. (F) Looking west at a steeply dipping forelimb of a fold in bedded sandstone layer of the Babulu Formation. Fold vergence is toward the south, as in E. (G) Mélange with blocks of Eocene limestone (above notebook), basalt, sandstone, and greenschist. (H) Panorama of uplifted coral terraces near Aimau. U/Th age is from lower terrace. Bedded units are forereef deposits capped by coral in growth position.
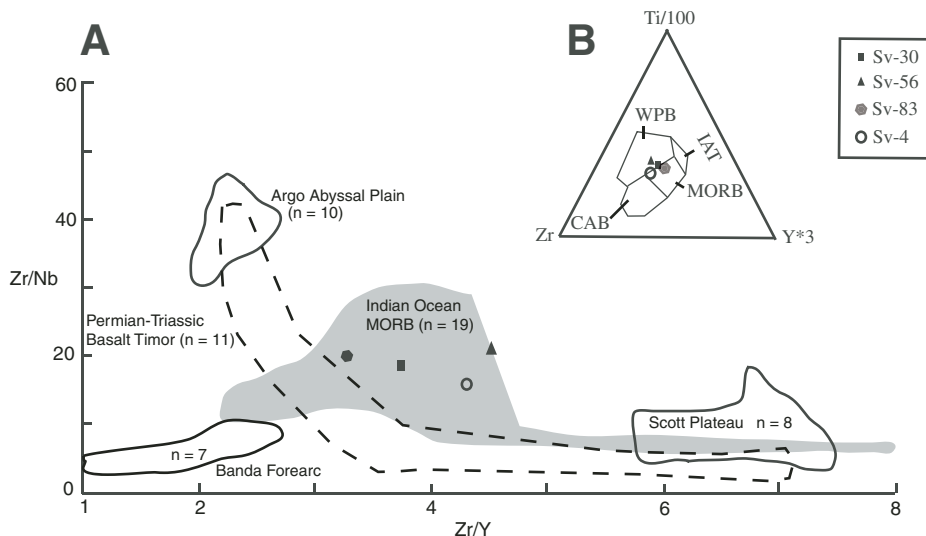

Figure 6. Geochemistry of Savu basalt. Sv-83 and Sv-4 are samples from the largest occurrence of basalt, which is in northern Savu and surrounded by mélange. Sv-30 and Sv-56 are from basalt interlayered with the Wai Luli Formation (Fig. 5C). (A) High field strength trace element compositions for Savu basalt overlap Indian Ocean mid-oceanic ridge basalt (MORB) (Ludden and Dionne, 1992) and plot between Argo abyssal plain and Scott Plateau compositions (Crawford and von Rad, 1994), which all overlap with Permian–Triassic basalt units found in Timor (Berry and Jenner, 1982). There is no similarity with forearc basalt from the Savu Basin (Harris, 1992, 2006). (B) Savu basalt plots near the boundary of MORB and within-plate basalts (WPB) on the tectonic discriminate diagram of Pearce and Cann (1973). IAT—island arc tholeiite; CAB—calc-alkaline basalt.

nappes is a duplex thrust system of mostly Permian and Triassic Gondwana sequence units (Harris et al., 1998). We infer a similar structural style for the uplift of the Sumba Ridge in the Savu region. We project the southern edge of the Sumba Ridge beneath the highest topography on Savu because mélange exposed in this region includes blocks of Sumba Ridge lithologies (Fig. 5G).

Sunda-Banda Forearc Units

The Sumba Ridge is correlated with outcrops in Sumba (van der Werff et al., 1995b) and Timor (Harris, 2006) that expose forearc cover and basement of the Asian affinity Sunda-Banda arc. These units include deformed Cretaceous—Miocene arc-derived sedimentary and volcanic rocks, which overlie greenschist to amphibolite facies metamorphic rocks with Eocene cooling ages (Harris, 2006; Standley and Harris, 2009). The Savu #1 well (Fig. 7) encountered blocks with similar compositions to units of the Sumba Ridge. It stopped drilling at a depth of 1227 m in Cretaceous clastic units, which we infer may have been the top of

the Sumba Ridge, since there are no Cretaceous clastic units on the Scott Plateau.

Eocene carbonate is identified in Rai Jua (the island immediately west of Savu), and as blocks in mélange encountered by the Savu #1 well. The Rai Jua occurrences have *Camerina* and *Discocyclina*, which are also found in Eocene limestone on Sumba (Grady et al., 1983). In Sumba, Eocene limestone is interlayered with andesitic and dacitic volcanic flows and tuffs. The age and composition of these rocks are associated with the Great Indonesian Arc that precedes the Miocene to present Sunda-Banda arc-trench system (Rutherford et al., 2001). In Animation 1, the Banda terrane is represented by black plasticine.

Mélange

Mélange is found in a discontinuous belt on the northern edge of exposures of accreted Australian continental margin units (Figs. 3 and 4) and in the Savu #1 well on the north coast. Due to the mud-dominated matrix of the mélange, it is poorly exposed as rolling slopes with lag deposits of blocks of mixed litholo-

gies, including some that do not crop out on the island (Fig. 5G). The best exposure we found is in a stream cut bank 5 km west of Seba, where blocks of indurated sandstone (Triassic?), crinoid-rich limestone (Permian?), and sparse blocks of metamorphic and igneous rocks (Banda terrane?) float in a matrix of expandable scaly clay. Blocks are mostly subangular and as large as 4 m in diameter. Matrix material has characteristics similar to those of the mudstone facies of the Wai Luli Formation.

In the Savu #1 well, mélange is encountered twice below a repeated section of late Miocene–Pliocene deep-water chalk: it is found at a depth of 290–725 m, and again at 900–1224 m. In these intervals the well drilled through several different types of blocks, which include (1) coarsely crystalline limestone with large, late-early Miocene benthonic foraminifera (340–346 m); (2) carbonate with a rich assemblage of upper Eocene foraminifera (440–483 m); (3) Oligocene fauna associated with an interval of mixed pebbles that include slate, chlorite schist, and quartz veins (~944 m); and (4) Cretaceous clastic units at the bottom of the well (1227 m). All of these rock types are found
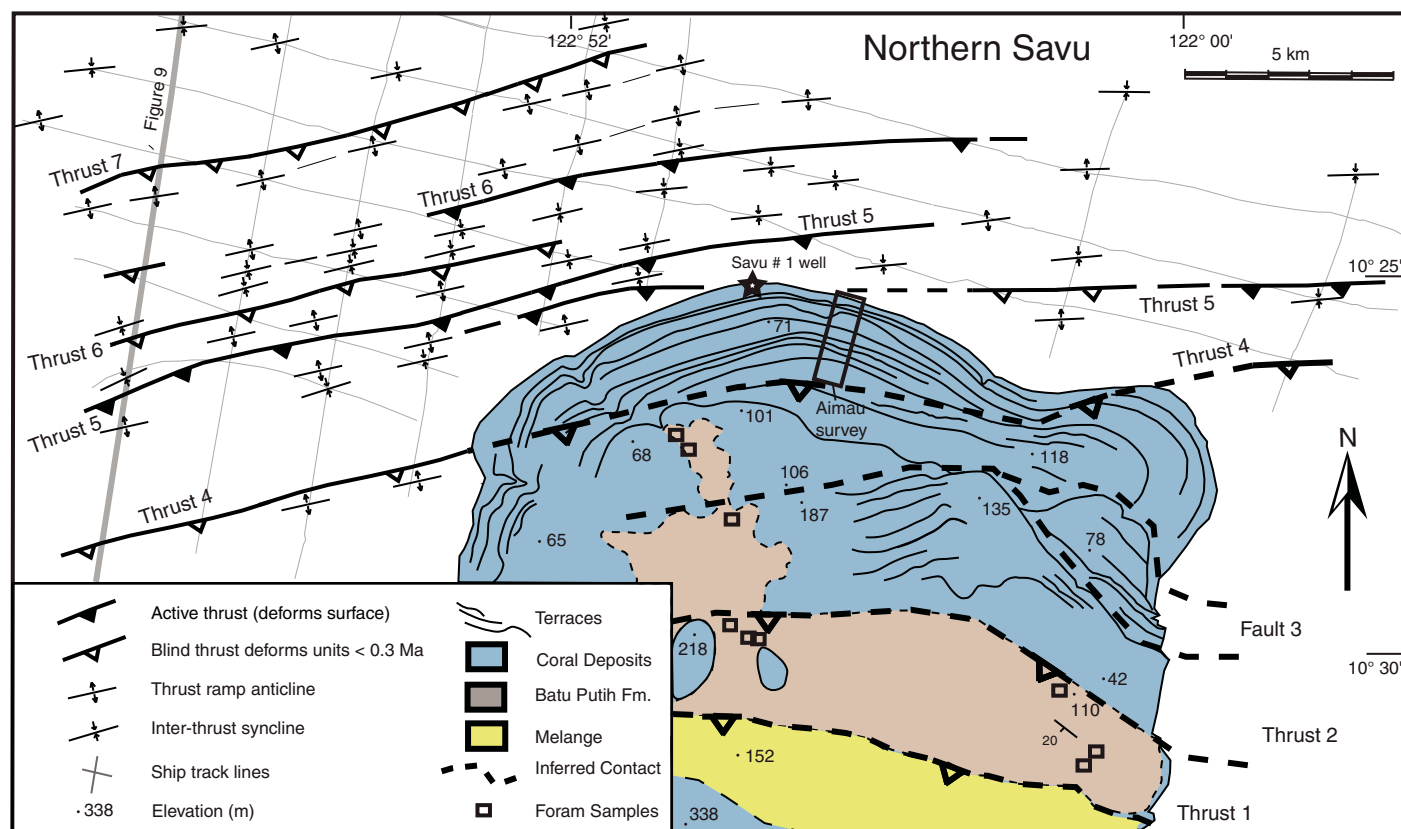
Figure 7. Structural map of northern Savu. Rectangle marks location of uplifted coral terrace survey (Fig. 10) near Aimau and star the location of the Savu #1 well. Gray lines are ship tracks of seismic reflection lines including Figure 9 on far left.

in the Banda terrane and have no Australian continental margin equivalent (Harris, 2006).

In southeastern Savu, mélange is locally found associated with active hot water mud volcanoes surrounded with lag deposits of basalt, crinoidal limestone, micrite, and sandstone, which have Australian continental margin associations. The highly altered basalt blocks have Ti, Sr, Zr, and Y contents similar to those of basalt interlayered with the Wai Luli Formation; this also supports a Wai Luli Formation source for much of the mélange. Mud volcanoes are also documented in seismic profiles north and west of Savu, near the toe of the accretionary wedge (Breen et al., 1986; Karig et al., 1987) and throughout Timor (Barber et al., 1987; Harris et al., 1998).

The structural position of mélange near the top of the Australian continental margin thrust stack and the degree of block rounding and mixing are similar to the Bobonaro mélange of the Timor region. The Bobonaro mélange is interpreted as forming along the suture between Asian affinity forearc thrust sheets above and a thrust duplex of Australian continental margin units below (Harris et al., 1998). A similar situation may exist in northern Savu.

Viqueque Group

The Viqueque Group of Timor (Audley-Charles, 1986a) represents a synorogenic sedimentary sequence that overlies rocks of the Sunda-Banda arc and Banda orogen. The basal Batu Putih Formation (Audley-Charles, 1968) is a pelagic chalk with some tuffaceous and calcilutite horizons that were deposited in the forearc basin, and over the southward-expanding accretionary wedge. Collision propagation from Timor to the southwest (Harris, 1991) predicts that ages of the upper Batu Putih Formation will vary throughout the region. In the forearc basin deposits exposed on Sumba (Fortuin et al., 1997), pelagic chalk (Waikabubak Formation) yields foraminifera ages as old as middle Miocene (N15) (all foraminifera zones and ages are according to Berggren et al., 1995; and geologic time scale [GTS2004] of Gradstein et al., 2005) and as young as latest Pliocene (N21, 3.35–1.92 Ma ago). In the accretionary wedge region of Timor (Audley-Charles, 1986a) and Savu (Roosmawati and Harris, 2009), the base of the Batu Putih Formation is latest Miocene (N18, 5.6–5.2 Ma ago); however, the age of the top of the unit youngs to the west (Roosmawati and Harris, 2009). In Timor the top is overlain by distal turbidites of N20, 4.20–3.35 Ma ago. In Rote and Savu there are no overlying turbidites, but pelagic chalk continues into the Pleistocene (Roosmawati and Harris, 2009). These

younger ages of the upper Batu Putih Formation reflect a much later uplift of these islands than indicated from the synorogenic sedimentary record of Timor.

The absence of turbiditic synorogenic units exposed on the islands west of Timor indicates the youth of islands where the initial stages of accretionary wedge emergence are observed. The part of the accretionary wedge exposed in Savu and Rote did not have a source for turbiditic sand. However, now that these islands are eroding it is likely that such deposits are accumulating in slope basins offshore.

The Batu Putih Formation in Savu consists mostly of foraminifera-rich, homogeneous white chalk. The chalk is interlayered locally with thinly bedded tuffaceous siltstone and marl. Pleistocene coral and fluvial gravels unconformably overlie the Batu Putih Formation (Fig. 5H). The thickest sections of the Batu Putih Formation exposed on Savu are >100 m thick, and are found mostly in the eastern part of the island (Figs. 3 and 7). The Savu #1 well encountered 240 m of chalk and calcilutite that overlies mélange. Ages from foraminifera in units drilled by the well indicate a disconformity at 63–70 m depth with N22/N23 (Pleistocene-Holocene) calcilutite intermixed with coral debris directly overlying N19 (4.2–5.2 Ma ago) age calcilutite (Fig. 5H). The base of the Batu Putih in the Savu #1 well is lower N18/N19 (5.6–5.0 Ma ago).

Detailed analysis of foraminifera of the Batu Putih Formation in outcrop (Roosmawati and Harris, 2009) indicates that the oldest units have a well-preserved assemblage of *Globorotalia tumida tumida* and *Globorotalia merotumida*, characteristic of Zone N18/N19 (5.6–5.0 Ma ago). Although the sections studied on Savu have similar ages to those sampled by the well, the faunal assemblages are slightly different. Outcrop ages near the top of the section are mostly N21 (3.35–1.92 Ma ago), which is determined by the first appearance of *Globorotalia tosaensis* and the last appearance of *Sphaeroidinellopsis seminulina seminulina* and *Globorotalia multicamerata*. The highest samples in the section have *Globorotalia truncatulinoidses*, *Globorotalia crassaformis*, and *Neogloboqudrina dutertei* that indicate an age of upper N21 and lower N22 (3.0 to younger than 1.92 Ma ago). N22/N23 ages were found at a depth of 55–63 m underlying and intermingled with Quaternary coral in the Savu #1 well.

Vintage seismic lines shot in the mid 1970s along the north coast of Savu (donated by International Oil) show continuous high-amplitude reflections of cover sedimentary units over acoustic basement (Fig. 8). Observations from the Savu #1 well and our mapping indicate that

this sedimentary section is the offshore equivalent of the Batu Putih Formation. Sediment thickness estimates of as much as 1000 m from seismic profiles are calculated using P-wave velocities of 1900–2300 m/s, which are reported for the uppermost sequence in the Savu Basin (van der Werff, 1995a).

Applying age data for the Batu Putih Formation that we report here also provides a way to estimate sedimentation rates, which is necessary for defining the age and duration of deformational events affecting the Batu Putih Formation. Strong bottom currents throughout the region have stripped sediments down to consolidated bedrock in places (Reed et al., 1986). However, successions as much as 1000 m thick accumulated in 5.6 Ma, which is a sedimentation rate of 178 m/Ma. The 240-m-thick section drilled and dated in the Savu #1 well yields sedimentation rates of 171 m/Ma. Two unconformities identified in the well indicate that this is a minimum rate. These rates are slightly higher than modern sedimentation rates measured in the Timor Trough of 140 m/Ma (Ganssen et al., 1989).

The maximum age of the Batu Putih Formation implies that the part of the accretionary wedge these sediments overlie formed by at least 5.6 Ma ago. The contact between accreted units and the overlying Batu Putih Formation is exposed in many places on the islands of Sumba, Savu, Rote, and Timor. In the forearc basin region of Sumba the basal age of chalk deposits is around the same as the age of volcanic arc itself (ca. 10 Ma old; Abbot and Chamalaun, 1981). The Batu Putih Formation in Savu and Timor has the same basal age of N18 (5.6 Ma old), which we interpret as the time that this part of the accretionary wedge formed.

Quaternary coral unconformably overlies most of the units of Savu (Fig. 5A). Coral terrace deposits are grayish-blue to white, and are commonly covered with a thin red soil. Flights of coral terraces are found in northern Savu as high as 338 m in elevation. The most complete section of terraces is well exposed on the north coast of Savu near Aimau (Figs. 5H and 8), which we surveyed and analyzed (see discussion of uplift history for results). At the base of some terraces is a conglomerate with calcilutite, sandstone, limestone, and micrite clasts.

STRUCTURE AND NEOTECTONICS

Analyses of structural features in Savu provide information for reconstructing its structural evolution and geometry. Combining these data with our studies of the recent history and patterns of uplift and subsidence of the island provide additional information. Savu and Rai

Jua form the top of an east-northeast–west-southwest ridge that parallels the structural grain of the northwest Australian continental margin. Extensional structures of the passive margin initiated in the late Paleozoic and continued throughout the Mesozoic until seafloor spreading moved the rift access away from the margin ca. 155 Ma ago (Symonds et al., 1998). Several rift basins formed that are mostly oriented east-northeast–west-southwest (Keep et al., 2002). As the continental margin encroaches upon the Sunda-Banda arc, some of these rift basins are inverted to form anticlines with fold axes oriented parallel to east-northeast–west-southwest rift basins (Doré and Stewart, 2002).

In many ways, the Savu–Rai Jua ridge can also be considered an inverted rift basin of the Scott Plateau; bedding attitude measurements throughout Savu show a dominantly east-northeast–west-southwest strike, which is also the orientation of fold hinge lines and thrust faults (Fig. 3). Based on these observations we claim that the pattern of deformation in Savu is strongly influenced by structural inheritance rather than the convergence direction, or the irregular orientation of the thrust front. In more advanced stages of collision south of Timor, the thrust front also rotates to parallelism with the structural grain of the northwest Australian continental margin (Fig. 1).
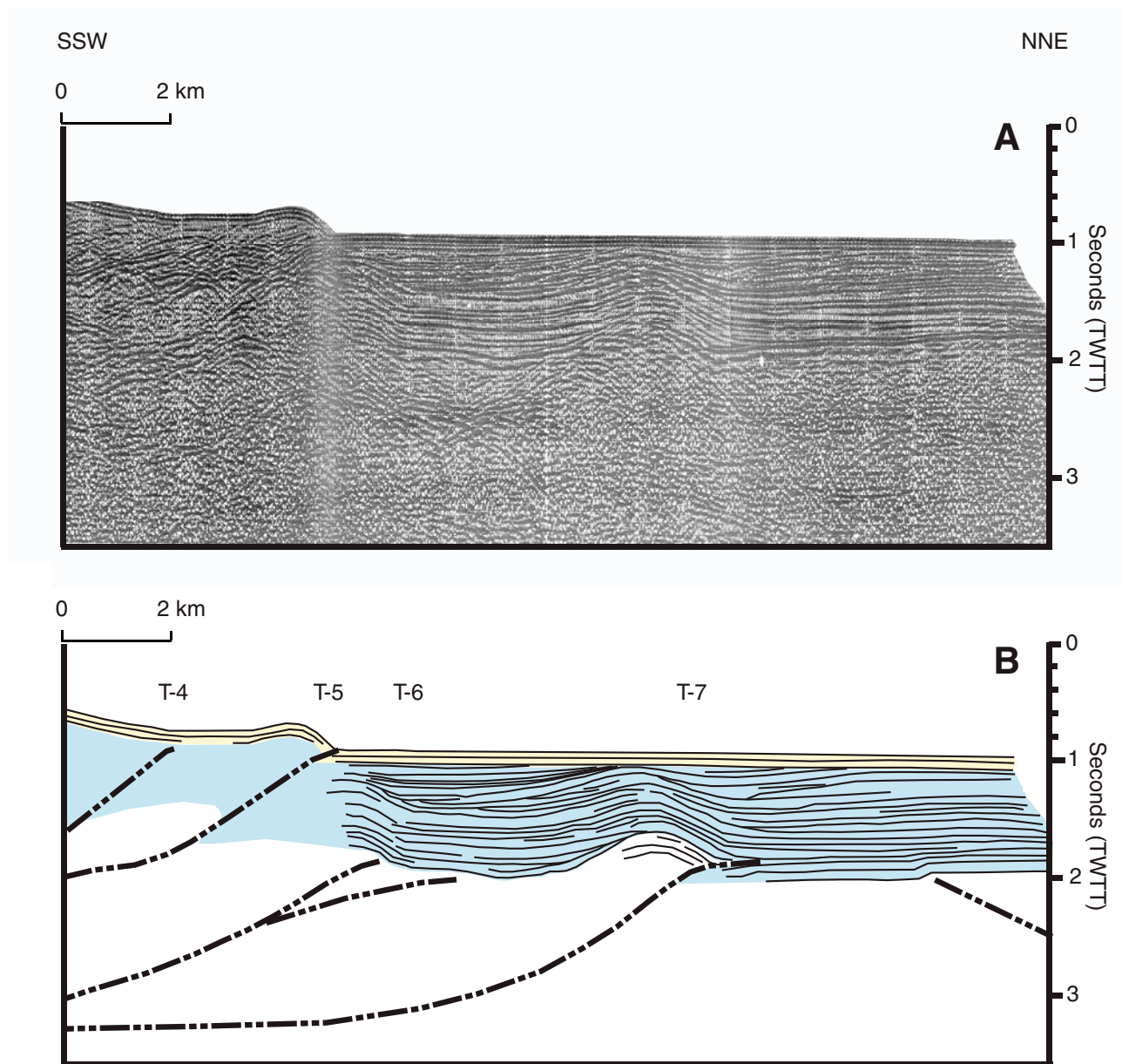
Figure 8. Seismic reflection profile shot off northwest coast of Savu in 1975 by International Oil. (A) Unmigrated record section. (B) Interpreted section showing deformed Batu Putih Formation (blue) and inferred thrust faults (T). Sedimentation rate is determined based on velocities of 2100 m/s. Folds show onlapping (growth) from ca. 2 Ma ago to present. However, the top 150 m of the profile is obscured by bubble pulse bottom reflectors (yellow). TWTT—two-way traveltime.

Cross Section

The composite north-northwest-south-southeast cross section (Fig. 9) of central Savu combines stratigraphic and structural relations mapped out on the island, encountered in the Savu #1 well, and imaged in seismic reflection profiles offshore. Starting in the offshore north of Savu, seismic data document a system of north-directed thrust faults of Pleistocene age (Figs. 7 and 8). The Savu #1 well reveals that these faults place mélange over the Batu Putih Formation. Drilling near the south coast of Timor documented >2 km of mélange beneath the Batu Putih Formation (Audley-Charles, 1986a). Block compositions from the well and in mélange outcrops in Savu and Rai Jua reveal a significant component of Sumba Ridge forearc material, which indicates that the southern edge of the Sunda-Banda forearc most likely extends beneath these outcrops. It is possible the Savu #1 well encountered the top of the forearc at its total depth of 1227 m. Seismic images off the north coast of Savu indicate that forearc basement is within 1400 m of the sea surface at the axis of the Sumba Ridge (Reed et al., 1986). In our cross section we have inferred a slightly deeper top adjacent to the Savu thrust system.

Movement of the Savu thrust system is young enough to deform even the youngest coral terraces (younger than 120 ka). Where erosion has stripped most of the coral canopy we find north-verging fold asymmetry in the northernmost exposure of Pedaro sandstone. We interpret this thrust sheet as the highest structural level of the Savu thrust system. In the backlimb syncline of this thrust are remnants of a coral terrace at 293 m elevation.

The central and southern parts of Savu provide excellent laterally continuous exposure of Australian continental margin units accreted to the edge of the Sunda forearc (Figs. 5A–5D). Our structural studies of these units identified three thrust-repeated sections of mostly Upper Triassic and Jurassic Australian continental margin units that are ~2 km thick. We infer that most lower Cretaceous and younger units are part of the roof thrust above the duplex system of Middle Triassic to Jurassic rocks. Most rocks incorporated into the duplex system dip north and form two different dip domains that represent a gently dipping top limb (20°–30°) and more steeply dipping (40°–50°) back limb of folds associated with south-directed thrusting. Some steeply dipping (Fig. 5F) and even overturned (Fig. 5G) forelimbs are found, but mostly as parasitic folds. No hanging-wall or footwall cutoffs, which are needed to estimate amounts of slip, are identified except on parasitic folds. However, the lack of any older parts of the Gondwana sequence between the thrust sheets indicates that they detach near the Middle Triassic and form a duplex beneath younger units and mélange (Animation 1). These data are also consistent with the relative thinness of thrust sheets and informs us that there are likely multiple detachments and zones of duplexing within the Gondwana sequence, as found in the Timor region (Harris, 1991).

The cross section indicates that two major geological domains divide Savu: the north is dominated by mélange, and synorogenic deposits overlying the edge of the Sunda-Banda forearc, and the south is dominated by accreted fragments of the Australian continental margin.
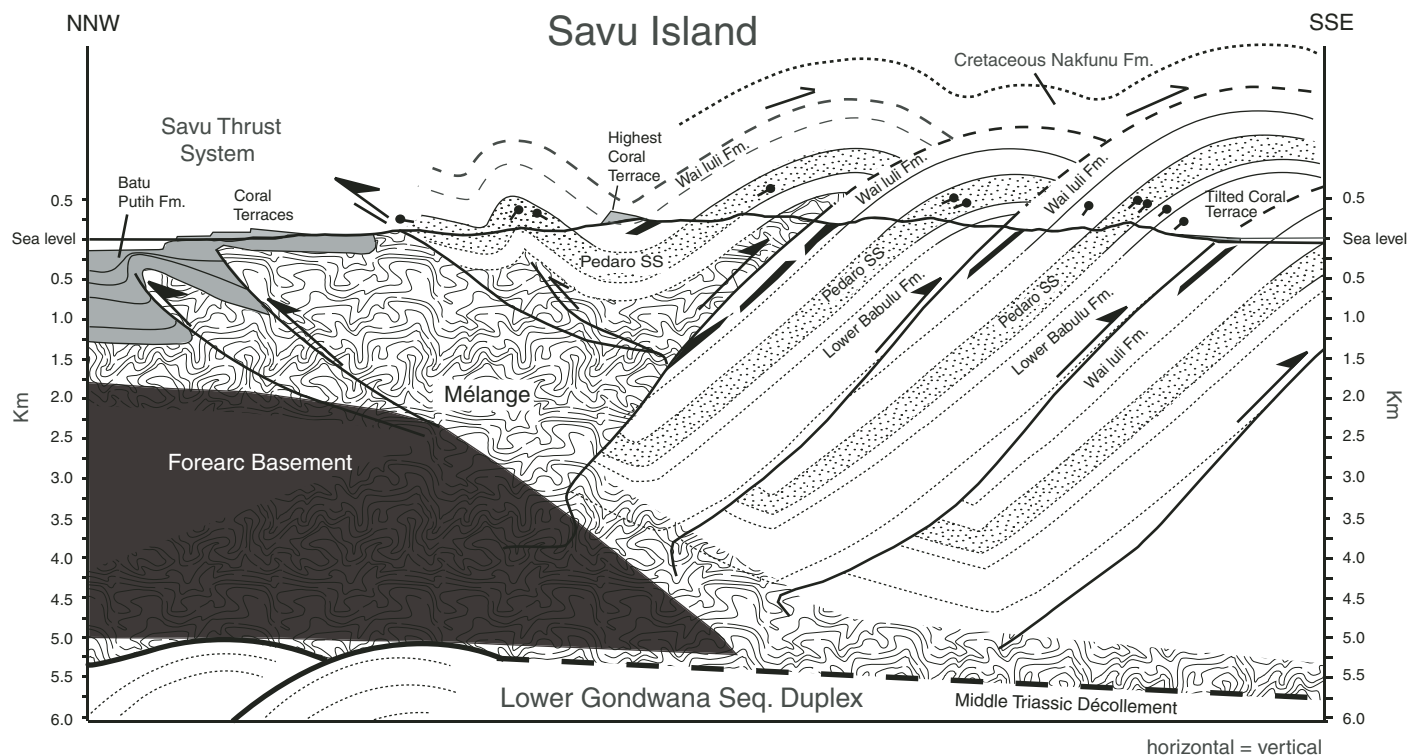
Figure 9. Composite north-northwest–south-southeast section across Savu (see Fig. 3 for line of section). **The structure of northern section is according to seismic profiles off the north coast and from drilling data. Folds and thrust faults are determined from field mapping (Fig. 3). Dip measurements are given by black dots with line pointing in direction of dip. Black bodies in Wai Luli Formation are basalt. Detachment depth is estimated from the projected depth of the Sumba Ridge and stratigraphic thickness of units incorporated into thrust sheets. Cretaceous units are interpreted as a roof thrust for the Upper Triassic–Jurassic duplex. Assuming no subduction erosion, the southern edge of the forearc was the precollisional Sunda-Banda trench, which is now abandoned due to accretion of Australian continental margin in front and beneath it. SS—sandstone; Seq.—sequence.**

The area between the two is a nascent collisional suture zone. Along orogenic strike in Timor, the suture zone is exposed at deeper structural levels (Harris et al., 1998). Several fragments of the Sunda-Banda forearc (Banda terrane) structurally overlie a duplex system of mostly Permian and Triassic Gondwana sequence units accreted from the edge of the Australian continental margin. Thick occurrences of mélange mark the mostly low-angle suture zone between arc and continental affinity units (Harris et al., 1998). This same suture zone in also recognized in Savu, where the rear of the accretionary wedge impinges upon and overrides the Sumba Ridge and Savu Basin along the Savu thrust.

Savu Thrust System

The Savu thrust is part of a system of at least four south-dipping thrust faults imaged by seismic studies between Savu and Sumba (Silver et al., 1983; Reed et al., 1986; Karig et al., 1987; van der Werff, 1995b). In the context of these other thrust faults, the Savu thrust is the northernmost of what may be interpreted as a forward-propagating thrust sequence from south to north. In front of the thrust faults are diapirs rising from acoustic forearc basement that are as much as 2 km across (van Weering et al., 1989). Seismic images of the faults show hundreds of meters of undeformed sedimentary successions overlying fault tips consistent with no slip at least during the late Quaternary (Silver et al., 1983). Although there is shallow seismic activity in the region, none has been directly attributed to the Savu thrust system (McCaffrey et al., 1985). The age of initiation of the Savu thrust system is unknown, and whether the fault is still active is debated (McCaffrey et al., 1985; Reed et al., 1986). The easternmost strand of the Savu thrust is projected through northern Savu and offshore to the east, where it dies out before it reaches the islands of Rote and Timor (Crostella and Powell, 1976; Reed et al., 1986).

To better understand the Savu thrust system we investigated the onshore and offshore regions of the north coast where it is projected into Savu. The Savu #1 well and structural field mapping of northern Savu demonstrates long-term north-directed thrusting. The tight seismic grid (Fig. 7) shows that most structural features are generally oriented east-northeast–west-southwest, subparallel to the structural grain of the Scott Plateau and Australian continental margin to the east.

Geomorphic patterns provide evidence of Pleistocene deformation along the northern part of Savu. Mélange is thrust northward over Batu Putih Formation units along thrust 1. Thrust 2 places Batu Putih Formation over coral deposits

with inferred ages of 780–850 ka, and other Batu Putih Formation units with younger foraminifera. Fault 3 is mapped on the basis of abruptly truncated and tilted coral terraces, but its sense of shear is unclear. Thrust 4 projects onshore from seismic reflection profiles on either side of Savu (Fig. 8) and may also account for the abrupt scarp that cuts across terraces at ~100 m elevation near the Aimau traverse (Fig. 7). These structural relations also indicate Pleistocene activity along the Savu thrust.

The International Oil seismic grid shot offshore (Fig. 7) shows thrust faults breaking to the surface and creating seafloor topography, which indicates Holocene displacement along the Savu thrust. Movement along thrust 5, as predicted by GPS results (Nugroho et al., 2009), produces as much as 250 m of vertical offset on the seafloor (Fig. 8). This structural relief increases eastward to 550 m west of Savu #1, then decreases farther east. The topography of the north coast of Savu mimics this pattern, suggesting a direct link between topography and recent movement along the Savu thrust. The Savu #1 well may have penetrated thrust 5, which could intersect the thrust fault found in the well if it dips ~30° south.

Combined movement along blind thrusts 6 and 7 deform well-imaged sections of the offshore equivalent of the Batu Putih Formation all of the way to the seafloor. The transition from predeformational to syndeformational units (constant thickness versus onlapping) is difficult to resolve with both folds. However, the extent of obvious onlapping units indicates that these folds may have been active for at least 1–2 Ma. However, most structures show little to no indication of growth, indicating they are very young and activated <1 Ma ago.

Using the line length of various reflections that can be traced over folds, we calculate a minimum rate of shortening over the past 1 Ma of 3.3 mm/a. This rate is a minimum estimate because only the deformation associated with folding is represented, not the total slip along faults. GPS baselines measured across the widest part of the Savu Sea in the direction of thrust transport show there is 6–8 ± 0.9 mm/a of convergence between Savu and western Flores (Nugroho et al., 2009). The Savu thrust system is the only structure identified along the baseline.

On either side of the Savu Sea there is evidence of greater amounts of closure of the Sunda-Banda forearc. For example, the Savu Sea ends to the west due to deformation in the Sumba region, where active thrust faults are inferred based on seismic reflection profiles (van der Werff et al., 1995a) and extensive flights of uplifted coral terraces (Pirazzoli et al., 1993). Age analysis of the coral indicates uplift rates of at least 0.5 mm/a during the past 1 Ma,

consistent with a shortening rate of ~3–4 mm/a, which is six times the rate of uplift.

The eastern part of the Savu Basin disappears where it is buried by north-directed thrust faults of the Timor orogenic wedge. Off of the west coast of West Timor a sequence of north-directed thrusts is similar to thrusts west of Savu, some of which break to the seafloor surface (Karig et al., 1987; van der Werff, 1995b). Farther to the east the thrust system causes the nearly complete closure of the forearc basin, and brings accreted Australian continental margin deposits to within 20 km of the Banda arc island of Atauro (Harris, 1991; Snyder et al., 1996). All along the north coast of East Timor are extensive flights of Pleistocene coral terraces with estimated uplift rates of ~0.5 mm/a (Chappell and Veeh, 1978). Many of the terraces are warped by short (10–15 km) wavelength folds indicating shallow crustal deformation processes (Cox et al., 2006), similar to those observed along the Savu thrust.

UPLIFT HISTORY

The emergence of Savu from a precollisional forearc ridge at depths of 3000–4000 m below sea level to an island as much as 340 m above sea level is recorded by thermal history indicators in uplifted Triassic units, depth versus age analysis of benthic and planktonic foraminifera in synorogenic deposits (Roosmawati and Harris, 2009), uplifted coral terraces, and patterns of longitudinal stream profiles. These different records yield uplift rate and deformation pattern information from different spatial and temporal scales. For example, analyses of thermal history indicators and foraminifera record uplift of the forearc ridge over a time span of 1–5 Ma, whereas coral terraces record uplift from approximately sea level to 300 m during only the past 50–800 ka. Records over such a broad range of time in an active orogen afford the rare opportunity to connect patterns of deformation found in bedrock units with their Pliocene–Pleistocene synorogenic sedimentary cover.

Thermal History Indicators

Vitrinite reflectance measurements of carbonaceous shale and mudstone indicate submature maximum paleotemperatures for Triassic and Jurassic units accreted from the Scott Plateau (Fig. 4). This contrasts with slightly higher vitrinite reflectance values found in age-equivalent units in Timor (Harris et al., 2000). The differences can be explained by the little to no postrift passive margin sediment overlying Gondwana sequence units of the Scott Plateau (Symonds et al., 1998) versus the northwest Australian continental margin accreted to

Timor. The Cretaceous–Pliocene sections on the continental slope that collided with Timor are at least 1.0–1.5 km thick.

Low vitrinite values also rule out heating associated with tectonic burial during accretion. A large scatter of apatite fission track ages and uniformly short track lengths found in Triassic units accreted to Timor (Harris et al., 2000) demonstrate that most of these units were in the partial annealing zone (>110 °C) before they were accreted, and were uplifted to the surface before new tracks formed (Harris et al., 2000).

Depth Versus Age Analysis of Foraminifera

Analysis of thousands of foraminifera from Batu Putih Formation chalk samples (see sample locations; Fig. 7) provide a way to define long-term depth versus age histories of synorogenic sedimentary units deposited over the Savu accretionary wedge (Roosmawati and Harris, 2009). All samples have both benthic and planktonic foraminifera, which provide a rough estimate of depth and age, respectively, of the Batu Putih Formation throughout Savu (Fig. 9). However, most samples consist of <2% benthic foraminifera, which is characteristic of abyssal depths (Van Marle et al., 1987).

Nearly all samples from Savu of N18 to N21 age (5.5–1.9 Ma ago) yield deep-marine benthic foraminifera (Fig. 10). Most of these show evidence of dissolution and low diversity with only the most dissolution-resistant species remaining (Roosmawati and Harris, 2009). Dissolution in the lysocline is found at depths of ~4000 m in Indonesia (Van Marle et al., 1987).

Some late N21 and early N22 samples near the top of the chalk show greater species diversity with little to no evidence of dissolution. We interpret this shallowing-upward trend as a consequence of slow uplift of the accretionary wedge between 5.5 and 1.0 Ma ago. Although the resolution is poor, these deposits were not uplifted more than 1500 m (0.5 mm/a) during this time interval, on the basis of the occurrences of *Globorotalia truncatulinoides*, of N22 (1.92 to 0.7 Ma), along with characteristic deep-water species, such as *Pullenia bulloides*, *Oridorsalis umbonatus*, and *Palnulina wuellerstorfi*. These deep-water benthic foraminifera indicate that deep conditions similar to the crest of the precollisional Lombok accretionary wedge to the west (3–4 km) persisted during N22.

An unconformity overlies the deep-water section of the Batu Putih Formation where much of zones N21 and N22 are missing. Above the unconformity are late N22/N23 (younger than 1 Ma) neritic species (0–200 m depth) intermingled with coral (Roosmawati and Harris, 2009). These relations indicate that after 1.92 Ma ago,

the rear of the Sunda-Banda forearc accretionary wedge was abruptly uplifted from a depth of ~2500–4000 m to near the surface before N22/N23. Surface uplift rates of 2–4 mm/a are required to get the accretionary wedge to the surface over such a short time interval (Fig. 11). This abrupt increase in uplift rate followed by slowing indicates to us that the accretionary wedge encountered an abrupt bathymetric feature such as the transform faulted northeast edge of the Scott Plateau, which has a relief of 2–3 km. Emergence of the island above sea level is well documented by flights of uplifted Pleistocene coral terraces that overlie the Batu Putih Formation.

Uplifted Coral Terraces

Coral terraces mostly surround the island of Savu, and cap its highest ridges to 338 m in elevation (Figs. 7 and 11A). These terraces provide a nearly continuous record of sea level

relative to the land surface that we use here to track rates and patterns of deformation during the Pleistocene. We surveyed uplifted coral terraces on both the north and south coasts of Savu (Fig. 11B), and analyzed U/Th ages of pure aragonite samples from these sections. The samples were first analyzed by X-ray diffraction for degree of alteration from aragonite to calcite. Five samples with ≥99% aragonite were found. However, four of these are from the centers of *Tridacna* shells, which yielded unreliable ages due to highly variable U values.
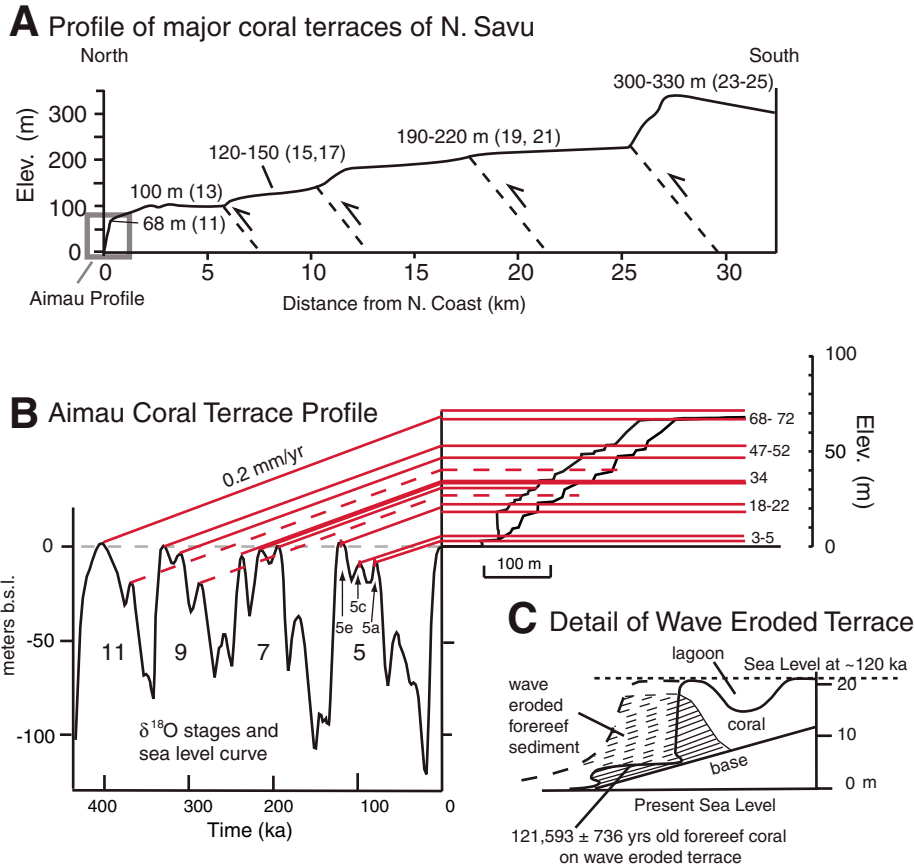
The only acceptable age is from coral on the north coast collected from an erosional terrace 4 ± 1 m above sea level (high tide mark – tidal range/2). It has an age of 121,593 ± 736 a (Table 2). This age corresponds to the beginning of the last major interglacial sea-level highstand (MIS 5e), which at that time was ~0–5 m above where it is now (Lambeck and Chappell, 2001). Although the coral most likely grew 3–4 m below sea level, at face value, this result indicates
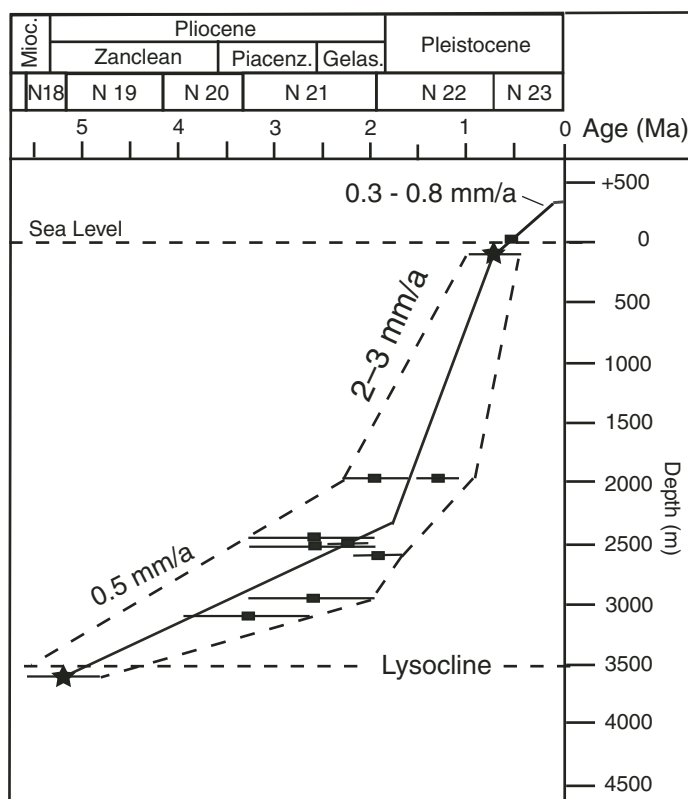
Figure 10. Surface uplift rates from depth versus age analysis of foraminifers. Each sample is represented by its upper depth limit (filled rectangle) based on benthonic foraminifers, and age range (horizontal line) based on planktonic foraminifers. The combination of these data provides minimum surface uplift rates. Parts of the curve above sea level are fixed by U-Series age analysis of uplifted coral terraces. Stars are data from the Savu #1 well.

that there is little uplift on the north coast relative to sea level since at least 121,593 a ago. However, stratigraphic analysis of the erosional terrace demonstrates that it is carved into bedded forereef sediments shed from a higher reef complex (Figs. 5H and 11C). Above the forereef sediment is a coral rampart in front of a lagoon 4–6 m deep. The architecture of the uplifted terrace is consistent with a single reef complex at least 20 m thick that was shedding coral from the barrier ridge down a forereef slope (Fig. 11C). Sea level at the time the reef was formed (stage 5e, ca. 122 ka ago) was at least as high as the top of the coral rampart, which varies from 18 to 22 m in elevation (Fig. 11). Wave action, from subsequent sea-level highstands (stage 5c and 5a, or stage 3), is responsible for eroding into the thick stage 5e coral reef as it was uplifted. The wave-cut terrace is also uplifted and warped, indicating recent deformation.

Holocene terraces associated with the present highstand are as much as 1150 m in width off of Point Bali (Fig. 7), but <100 m wide on the north coast. A similar pattern is found in the more than 20 uplifted terraces above the present coral reef. Matching coral ages with elevations yields a best-fit minimum uplift rate solution of 0.2–0.3 mm/a (Fig. 11B). At this low rate, some lower highstands (dashed) are in the shadow of later higher ones, and may only be represented by small notches, such as those found in stages 9 and 11. The profile across the northern part of Savu (Fig. 10A) shows some very wide terraces at 100 m, 130–150 m, 180–220 m, and 300–330 m. The minimum uplift rate of 0.2 mm/a provides a poor match between known sea level high-stands and terrace elevations above 68–72 m. Higher uplift rates of at least 0.4–0.5 mm/a are needed to fit broad terraces with major isotope stages (Fig. 11A). The match of sea level high-stands

A Profile of major coral terraces of N. Savu

B Aimau Coral Terrace Profile

C Detail of Wave Eroded Terrace

121,593 ± 736 yrs old forereef coral on wave eroded terrace

Figure 11. Profiles of uplifted coral terraces on the north coast of Savu near Aimau (see Fig. 7 for location). (A) Profile from coast to highest terrace with elevations and inferred oxygen isotope stages. Thrust faults correlate with those in Figure 7. (B) Detail of lowest part of profile A correlating terraces with sea-level highstands according to U/Th age of lowest surface (3–5 m) (b.s.l.—below sea level). Assuming constant uplift yields a best-fit correlation of 0.2 mm/a. (C) Detail of lowest terraces in B. Terrace at 3–5 m is a wave-eroded platform cut into the stage 5e terrace, exposing forereef sediments. Eroded parts of reconstructed forereef are shown (dashed).

TABLE 2. ^{230}Th DATING RESULTS

Sample number	^{238}U (ppb)	^{232}Th (ppt)	^{230}Th / ^{232}Th (atomic x 10^{-6})	δ^{234}U* (measured)	^{230}Th / ^{238}U (activity)	^{230}Th age (yr) (uncorrected)	^{230}Th age (yr) (corrected)	δ^{234}U$_{initial}$† (corrected)
7/23/01BR#2B	1692 ± 2	12281 ± 24	1706 ± 6	99.8 ± 1.4	0.7497 ± 0.0023	121778 ± 732	121593 ± 736	140.7 ± 2.0
7/24-2C#1	32.4 ± 0.1	276 ± 6	1672 ± 36	149 ± 13	0.8635 ± 0.0044	144619 ± 4060	144416 ± 4052	224 ± 20
7/24-2A-I	229.4 ± 0.3	652 ± 7	5941 ± 64	150.5 ± 2.3	1.0226 ± 0.0043	215180 ± 3052	215116 ± 3050	276.5 ± 4.9
7/24-2A-II	230.1 ± 0.2	632 ± 7	6132 ± 66	148.2 ± 1.7	1.0210 ± 0.0029	215716 ± 2135	215653 ± 2134	272.7 ± 3.5
7/30-1A	2033 ± 3	73652 ± 521	7.0 ± 0.3	147.1 ± 1.7	0.0154 ± 0.0007	1476 ± 64	554 ± 468	147.3 ± 1.8
7/23-3D	167.6 ± 0.2	237 ± 5	10958 ± 246	104.8 ± 2.2	0.9367 ± 0.0045	193309 ± 2759	193274 ± 2758	180.9 ± 4.1

*δ^{234}U = [(^{234}U / ^{238}U) activity − 1] x 1000.

†δ^{234}U$_{initial}$ was calculated based on ^{230}Th age (T), i.e., δ^{234}U$_{initial}$ = δ^{234}U$_{measured}$ x e$^{\lambda234 xT}$.

Note: The error is 2σ. λ_{230} = 9.1577 x 10^{-6} y^{-1}, λ_{234} = 2.8263 x 10^{-6} y^{-1}, λ_{238} = 1.55125 x 10^{-10} y^{-1}. Corrected ^{230}Th ages assume the initial ^{230}Th / ^{232}Th atomic ratio of 4.4 ± 2.2 x 10^{-6}. Those are the values for a material at secular equilibrium, with the bulk earth ^{232}Th / ^{238}U value of 3.8. The errors are arbitrarily assumed to be 50%.

with terraces may also be complicated by thrust faults inferred on the basis of juxtaposition of different uplift patterns (Fig. 7).

All of the terraces we surveyed are laterally warped, with the highest elevations near and south of the Aimau region (Fig. 7). Terraces decrease slightly in elevation to the west, where they wrap around the northwest coast and change geometry abruptly above an elevation of ~30–40 m. The change corresponds with where thrust 3, which is found in offshore seismic profiles, intersects with the coastline (Fig. 7). We infer that thrust 3 tracks beneath the terraces and joins with another recently active thrust segment found off Point Bali at the eastern tip of the island. We also infer that the well-developed wide terraces on Point Bali are on the hanging wall of thrust 3. However, to the south, the broad terraces of Point Bali are truncated against older coral terraces that tilt eastward from 78 m elevation to sea level over a distance of only 3 km (Fig. 7). We infer a fault at this location to explain these discontinuities, but the sense of shear is not clear.

On the south coast of Savu, an extensive coral carapace is tilted seaward as much as 5° (Fig. 5A) from elevations of ~25 m to below sea level over a distance of 250–300 m. *Tridacna* shells found on this terrace did not produce reliable ages. However, the fact that the terrace is at least 25 m above sea level indicates that the south coast has also undergone some Pleistocene uplift. The lack of multiple flights of terraces, and the southward tilt into the sea, indicates that uplift was slow or short lived, and did not keep pace with the north coast.

The western coastal regions of Savu have coral terraces that dip as much as 8° westward beneath the narrow Rai Jua Strait between Savu and Rai Jua Islands. On the east coast of Rai Jua coral terraces are observed that dip ~5° eastward, back toward the strait. The corresponding dips on each side of the strait help us rule out slumping as a cause of the deformation. Instead, we interpret the deformation pattern as a result of differences in amounts of slip along strike of various segments of the Savu thrust. In this case, the strait may represent a fault segment boundary where the tips of two thrust faults end or slightly overlap, leaving a slip deficit.

In summary, we interpret the deformation pattern of coral terraces, with continuous uplift on the north coast, uplift followed by southward tilt on the south coast, and warping that corresponds to topography, as a result of activity along the Savu thrust system over the past 800 ka.
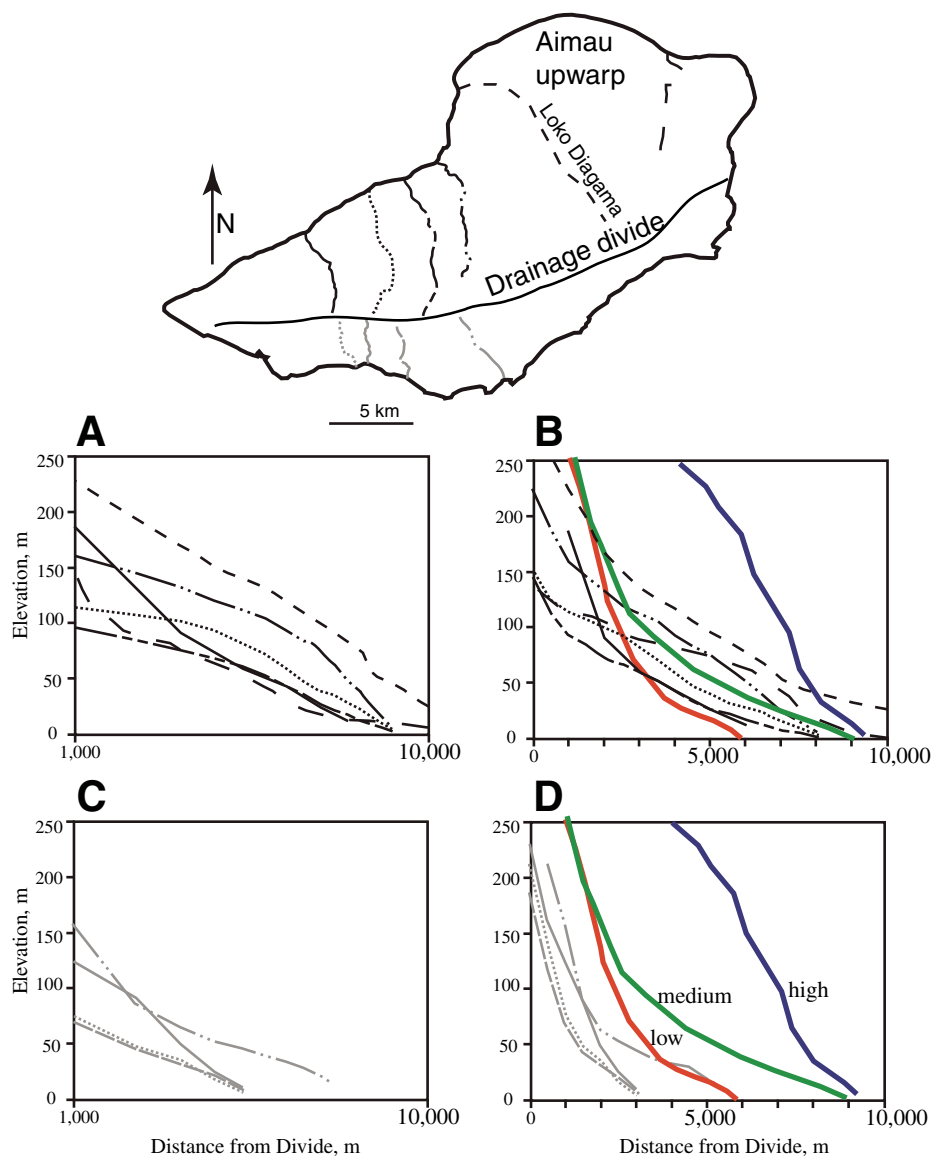
Stream Longitudinal Profiles

As Savu emerged above sea level, drainages developed in response to differential uplift across

the strike of the island. Longitudinal profiles from seven different rivers on Savu (Fig. 12) were produced from 1:25,000 topographic maps and plotted according to the method of Merritts and Vincent (1989). Stream gradient points were taken every 500 m from the coast to drainage divides.

Stream profiles differ on either side of the east-northeast–west-southwest—trending divide of Savu (Fig. 12). Rivers south of the divide show linear to slightly concave profiles

on elevation versus log distance from the divide. South-draining streams have lower order, high-gradient profiles. North-draining stream profiles show only one concave profile and the rest are distinctly convex. Stream gradients and degree of convexity generally increase toward the Aimau upwarp, where coral terraces also achieve their maximum elevations. In most drainages, differences in lithology show no detectable effect on stream gradient. Climate variation on the island

Figure 12. Longitudinal stream profiles of Savu. Various dashed lines correspond to locations of streams on map with black lines for streams north of the divide (A and B) and gray lines representing streams south of the divide (C and D). Data acquired every 500 m within drainages. Horizontal scales are semilogarithmic on left and arithmetic on right. Colored lines represent profile estimates of relative uplift rate (Merritts and Vincent, 1989). Plots show that uplift rates were high in the recent past along the south coast, but now only have low-order streams to base level. North-draining streams show intermediate uplift rates with some convex-shaped profiles.

is also negligible due to little to no rain shadow. We consider tectonics as the major variable controlling stream profile gradient and shape.

Comparisons of Savu stream profiles with other studies (Merritts and Vincent, 1989) indicate mostly medium rates of uplift north of the divide (Fig. 12), and those streams have significantly higher uplift rates than south-directed streams that show only evidence of past uplift (steep low-order stream gradients). The asymmetry of drainage basin length north and south of the divide also demonstrates higher rates of uplift to the north. Overall, the analysis of stream profiles corroborates other evidence for the northward advance of the Scott Plateau beneath Savu during the Quaternary.

COLLISION INITIATION AND EVOLUTION IN THE SAVU REGION

To estimate the timing of events that shaped Savu, we reconstruct the position of the Scott Plateau through time and compare it with the uplift history. We use the northeast edge of the Scott Plateau as a reference point, which corresponds with the axis of the Sumba Ridge ~10 km north of the Savu (Fig. 1). Palinspastic reconstruction of the position of the northeast edge of the Scott Plateau is possible because we know the convergence rate between it, the volcanic arc, and Savu. Long-term rates of convergence between Australia and Eurasia are estimated as 71 km/Ma at 014° (Kreemer et al., 2003). These rate estimates based on geological features are nearly identical to GPS measurements between Australia (Darwin) and Eurasia of 69 ± 0.3 mm/a at 016° (Nugroho et al., 2009). Both geological data and GPS measurements also document that the forearc and arc move north-northeast relative to Eurasia. Savu moves at a rate of 31 ± 1 mm/a and the western part of Flores at a rate of 23 mm/a (Nugroho et al., 2009). We infer that the difference in motion between Savu and western Flores (8 ± 1 mm/a) is the deformation rate on the Savu thrust system. The net motion of the Scott Plateau relative to Savu once it arrives at the Java Trench is 40 mm/a (71 mm/a – 31 mm/a). At this rate, the Scott Plateau would have arrived in southern Savu ca. 0.82 Ma ago and the north coast of Savu at 0.25 Ma ago.

In order to determine when the Scott Plateau first collided with the Sunda-Banda trench south of Savu, we reconstruct the position of the trench based on the consistent 290–305 km arc-trench distance of the eastern Sunda arc. At this distance from the active volcanic arc north of Savu, the trench would have been at latitude 11.2° to 11.4°S. The Sumba Ridge is 97–118 km from the inferred position of the Sunda-Banda trench

south of Savu (Fig. 1), which means that the Scott Plateau arrived at the trench ca. 1.3–1.7 Ma ago.

The collision of the Scott Plateau with the Sunda-Banda arc has also modified other features of the arc-trench system. For example, the distance between the forearc ridge crest and the arc is consistently ~230–240 km throughout the eastern Sunda arc, which is only 50–60 km from the trench (van der Werff et al., 1995b). At ~118°E (just west of Sumba) these distances begin to change. A distinct westward bend of the 5000 m depth contour of the lower plate is found. North of this shallower section of the lower plate, the Java trench and Savu accretionary ridge are indented ~40 km to the north (Fig. 1). Sumba rises in what was the forearc basin, and directly to the north of western Sumba the arc is inactive. In the backarc north of Sumba, the Flores thrust is also deflected northward >30 km (Silver et al., 1986). We interpret these features as modifications to the eastern Sunda arc by collision of the westernmost Scott Plateau protrusion that currently is underthrusting the Sunda forearc beneath Sumba (Fig. 1).

The estimated time of collision initiation at the Sunda-Banda deformation front and the observed collisional modifications to the arc-trench system are consistent with other results we present here, such as (1) foraminifera analyses that document rapid uplift from precollisional depths of a accretionary ridge to the surface later than 1.90 Ma ago, (2) uplifted coral terraces as old as 800 ka, (3) faults that offset these Quaternary deposits, and (4) an active fold-and-thrust belt tracking the northward progression of the Sumba Ridge.

The shape of the Australian continental margin changes south of Savu to a more north-northeast–south-southwest direction, which is nearly parallel to its convergence direction. This implies that the shelf-slope break that is currently colliding with West Timor will not arrive at the deformation front south of Savu for another 6.0 Ma. South of Sumba the Scott Plateau has already underthrust the Sunda-Banda forearc and now oceanic lithosphere is again subducting beneath the deformation front. The next part of the Australian continental margin to collide with Sumba will likely be the Exmouth Plateau, which has a large northwest-southeast–oriented crustal prong very similar to the Scott Plateau (Longley et al., 2002). During this event ~9–10 Ma from now, the arc-continent collision may extend as far as Bali, but the rest of the Sunda arc will most likely remain a subduction zone unless plate boundaries in the region reorganize.

In contrast, the configuration of the Australian continental margin south of West Timor (lower angle of collisional obliquity) results in very lit-

tle lag time between initial uplift ca. 3–4 Ma ago as the distal edge of the continental slope collided with the Sunda-Banda trench, and a later phase of rapid uplift signaling the arrival of the Australian shelf at the trench ca. 0.2 Ma ago (De Smet et al., 1990). Between these two pulses of uplift the accretionary wedge subsided. These along-strike variations in timing, and the episodic advance of the orogen that they cause, are very difficult to resolve in reconstructing older, more mature orogens. However, these events may explain some of the disparate ages of similar features and structural discontinuities in older orogens.

CONCLUSION

The Savu region provides a rare glimpse of neotectonic associations of the transition from subduction to collision. Complexities result from lower plate structural and stratigraphic discontinuities that cause waves of crustal shortening and uplift followed by subsidence. The geology of the Savu region is separated into two very different domains divided by a developing suture zone between units of Australian and Asian affinity. Australian affinity units correlate with the Gondwana sequence that is also found in Rote and Timor. Asian affinity units correlate with those exposed in Sumba and other parts of the Sunda-Banda arc, and high-level thrust sheets in Timor.

The shortening history of the Savu region involves thrust duplex development of mostly Triassic–Jurassic synrift Gondwana sequence sedimentary and volcanic rocks accreted from the subducting Scott Plateau by top-to-the-southeast thrusting. The direction of shortening is controlled by the inherited east-northeast–west-southwest structural grain of the Australian continental margin. The southern edge of the Sunda-Banda forearc forms the backstop of the accretionary wedge via the Savu thrust system. Increased coupling between the underthrust Scott Plateau and the overriding Sunda-Banda forearc actively drives the rear of the accretionary wedge northward over the Sunda-Banda forearc basin at rates of ~8 mm/a. This northward motion is accommodated by the active Savu thrust system, which offsets Quaternary deposits on the north coast and is well imaged by seismic reflection profiles offshore.

The uplift history of Savu documents the arrival and passing of the northeast edge of the Scott Plateau beneath the Savu region between 0.8 and 0.2 Ma ago. Foraminifera from synorogenic deposits reveal pelagic depths of 2.5–4.0 km between 5.6 Ma and more recently than 1.9 Ma ago. By roughly 1 Ma ago, neritic species were present that document uplift of the

synorogenic section to within 200 m of the surface in <1 Ma. By ca. 0.8 Ma ago, coral terraces formed in the central part of the island above the deepest structural levels of the exposed accretionary wedge. The island continued to grow northward at a rate of ~2 m/ka, as recorded by flights of uplifted coral. The youngest coral terraces are erosional features into the massive MIS 5e (122 ka) coral complex.

Savu Island documents that initiation of intra-forearc convergence, and partitioning of strain away from the deformation front, and is one of the earliest transitional phases from subduction to collision. Although this phase of deformation commonly occurs in subduction zones due to collision of seamounts and other lower plate obstructions, it signals the beginning of the end of subduction in the eastern Sunda-Banda arc. Similar phases of deformation occurred earlier both west and east of Savu Island due to the V-shaped geometry of the northeast-southwest Australian continental margin and the northwest-southeast protrusion of the Scott Plateau.

ACKNOWLEDGMENTS

REFERENCES CITED

Abbot, M.J., and Chamalaun, F.H., 1981, Geochronology of some Banda arc volcanics, *in* Barber, A.J., and Wiryosuyono, S., eds., The geology and tectonics of eastern Indonesia: Bandung, Indonesia, Geological Research and Development Center Special Publication 2, p. 253–268.

Audley-Charles, M.G., 1968, The geology of Portuguese Timor: Geological Society of London Memoir 4, 75 p., doi: 10.1144/GSL.MEM.1968.004.01.01.

Audley-Charles, M.G., 1985, The Sumba enigma: Is Sumba a diapiric forearc-nappe in process of formation?: Tectonophysics, v. 119, p. 435–449, doi: 10.1016/0040-1951(85)90049-6.

Audley-Charles, M.G., 1986a, Timor-Tanimbar Trough: The foreland basin to the evolving Banda orogen, *in* Allen, P.A., and Homewood, P., eds., Foreland basins: International Association of Sedimentologists Special Publication 8, p. 91–102.

Audley-Charles, M.G., 1986b, Rates of Neogene and Quaternary tectonic movements in the Southern Banda arc based on micropaleontology: Geological Society of London Journal, v. 143, p. 161–175, doi: 10.1144/gsjgs.143.1.0161.

Audley-Charles, M.G., 2004, Ocean trench blocked and obliterated by Banda forearc collision with Australian proximal continental slope: Tectonophysics, v. 389, p. 65–79, doi: 10.1016/j.tecto.2004.07.048.

Barber, A.J., Audley-Charles, M.G., and Carter, D.J., 1987, Thrust tectonics in Timor: Geological Society of Australia Journal, v. 24, p. 51–62.

Berggren, W.A., Hilgen, F.J., Langereis, C.G., Kent, D.V., Obradovich, J.D., Raffi, I., Raymo, M.E., and Shackleton, N.J., 1995, Late Neogene chronology; new perspectives in high-resolution stratigraphy: Geological Society of America Bulletin, v. 107, p. 1272–1287, doi: 10.1130/0016-7606(1995)107<1272:LNCNPI> 2.3.CO;2.

Berry, R.F., and Grady, A.E., 1981, Deformation and metamorphism of the Aileu Formation, north coast, East Timor and its tectonic significance: Journal of Structural Geology, v. 3, p. 143–167, doi: 10.1016/0191-8141(81)90011-0.

Berry, R.F., and Jenner, G.A., 1982, Basalt geochemistry as a test of tectonic models of Timor: Geological Society of London Journal, v. 139, p. 593–604, doi: 10.1144/gsjgs.139.5.0593.

Bird, P.R., and Cook, S.E., 1991, Permo-Triassic successions of the Kekneno area, West Timor: Implications for paleogeography and basin evolution: Journal of Southeast Asian Earth Sciences, v. 6, p. 359–371, doi: 10.1016/0743-9547(91)90081-8.

Bowin, C., Purdy, G.M., Johnston, C., Shor, G., Lawyer, L., Hartono, H.M.S., and Jezek, P., 1980, Arc-continent collision in the Banda Sea region: American Association of Petroleum Geologists Bulletin, v. 64, p. 868–918.

Breen, N.A., Silver, E.A., and Hussong, D.M., 1986, Structural styles of an accretionary wedge south of the island of Sumba, Indonesia, revealed by SeaMarcII side scan sonar: Geological Society of America Bulletin, v. 97, p. 1250–1261, doi: 10.1130/0016-7606(1986)97<1250:SSOAAW> 2.0.CO;2.

Brouwer, H.A., 1925, The geology of the Netherlands East Indies: Lectures delivered as exchange-professor at the University of Michigan in 1921–1922: New York, Macmillan, 160 p.

Carter, D.J., Audley-Charles, M.G., and Barber, A.J., 1976, Stratigraphical analysis of island arc-continental margin collision in eastern Indonesia: Geological Society of London Journal, v. 132, p. 179–198, doi: 10.1144/gsjgs.132.2.0179.

Chamalaun, F.H., and Grady, A.E., 1978, The tectonic evolution of Timor: A new model and its implications for petroleum exploration: Australian Petroleum Exploration Association Journal, v. 18, p. 102–108.

Chamalaun, F.H., Grady, A.E., von der Borch, C.C., and Hartono, H.M.S., 1982, Banda arc tectonics: The significance of the Sumba Island (Indonesia), *in* Watkins, J.S., and Drake, C.L., eds., Studies in continental marine geology: American Association of Petroleum Geologists Memoir 34, p. 361–375.

Chappell, J., and Veeh, H., 1978, Late Quaternary tectonic movements and sea-level changes at Timor and Atauro Island: Geological Society of America Bulletin, v. 89, p. 356–368, doi: 10.1130/0016-7606(1978)89<356:LQTMAS> 2.0.CO;2.

Charlton, T.R., 1991, Postcollision extension in arc-continent collision zones, eastern Indonesia: Geology, v. 19, p. 28–31, doi: 10.1130/0091-7613(1991)019<0028: PEIACC>2.3.CO;2.

Cox, N.L., Harris, R.A., and Merritts, D., 2006, Quaternary uplift of coral terraces from active folding and thrusting along the northern coast of Timor-Leste: Eos (Transactions, American Geophysical Union), v. 87, abs. T51D-1564.

Crawford, A.J., and von Rad, U., 1994, The petrology, geochemistry and implications of basalts dredged from the Rowley Terrace–Scott Plateau and Exmouth Plateau margins, northwestern Australia: AGSO Journal of Australian Geology & Geophysics, v. 15, p. 43–55.

Crostella, A.A., and Powell, D.E., 1976, Geology and hydrocarbon prospects of the Timor area: Indonesian Petroleum Association Proceedings, v. 2, p. 149–171.

De Smet, M.E.M., Fortuin, A.R., Troelstra, S.R., van Marle, L.J., Karmini, M., Tjokrosapoetro, S., and Hadiwasastra, S., 1990, Detection of collision-related vertical movements in the Outer Banda Arc (Timor, Indonesia), using micropaleontological data: Journal of Southeast Asian Earth Sciences, v. 4, p. 337–356.

Dickinson, W.R., Beard, L.S., Brakenridge, G.R., Erjavec, J.L., Ferguson, R.C., Inman, K.F., Knepp, R.A., Lindber, F.A., and Ryberg, P.T., 1983, Provenance of North American Phanerozoic sandstones in relation to tectonic setting: Geological Society of America Bulletin, v. 94, p. 222–235, doi: 10.1130/0016-7606(1983)94<222:PONAPS> 2.0.CO;2.

Dore, A.G., and Stewart, I.C., 2002, Similarities and differences in the tectonics of two passive margins; the Northeast Atlantic margin and the Australian North West Shelf, *in* Keep, M., and Moss, S.J., eds., Sedimentary basins of Western Australia: Petroleum Exploration Society of Australia Symposium Proceedings, v. 3, p. 89–117.

Fortuin, A.R., van der Werff, W., and Wensink, H., 1997, Neogene basin history and paleomagnetism of a rifted and inverted forearc region, on- and offshore Sumba, eastern Indonesia: Journal of Asian Earth Sciences, v. 15, p. 61–88.

Ganssen, G., Troelstra, S.R., Faber, B., van der Kaars, W.A., and Situmorant, M., 1989, Late Quaternary palaeoceanography of the Banda Sea, eastern Indonesia piston cores (Snellius-II Expedition, Cruise G5): Netherlands Journal of Sea Research, v. 24, p. 491–494.

Genrich, J.F., Bock, Y., McCaffrey, R., Calais, E., Stevens, C.W., and Subarya, C., 1996, Accretion of the southern Banda arc to the Australian plate margin determined by Global Positioning System measurements: Tectonics, v. 15, p. 288–295, doi: 10.1029/95TC03850.

Gianni, L., 1971, The geology of the Belu district of Indonesian Timor [M.Ph. thesis]: London, University of London, 122 p.

Gradstein, F.M., Ogg, J.G., and Smith, A.G., 2005, A geologic time scale 2004: Cambridge, Cambridge University Press, 610 p.

Grady, A.E., Abbott, M.J., Chamalaun, F.H., and von der Borch, C.C., 1983, The Banda Arc, Sumba to Timor: A review: Geological Society of Australia Journal, v. 9, p. 23–25.

Haig, D.W., McCartain, E., Barber, L., and Backhouse, J., 2007, Triassic–Lower Jurassic foraminiferal indices for Bahaman-type carbonate-bank limestones, Cablac Mountain, East Timor: Journal of Foraminiferal Research, v. 37, p. 248–264, doi: 10.2113/ gsjfr.37.3.248.

Haile, H.S., Barber, A.J., and Carter, D.J., 1979, Mesozoic cherts on crystalline schists in Sulawesi and Timor: Geological Society of London Journal, v. 136, p. 65–70, doi: 10.1144/gsjgs.136.1.0065.

Hamilton, W., 1979, Tectonics of the Indonesian region: U.S. Geological Survey Professional Paper 1078, 345 p.

Harris, R.A., 1991, Temporal distribution of strain in the active Banda orogen: A reconciliation of rival hypotheses: Journal of Southeast Asian Earth Sciences, v. 6, p. 373–386, doi: 10.1016/0743-9547 (91)90082-9.

Harris, R.A., 1992, Peri-collisional extension and the formation of Oman-type ophiolites in the Banda Arc and Brooks Range, *in* Parson, L.M. et al., eds., Ophiolites and their modern oceanic analogues: Geological Society of London Special Publication 60, p. 301–325.

Harris, R.A., 2004, Geodynamic patterns of ophiolites and marginal basins of the Indonesian and New guinea regions, *in* Dilek, Y., and Robinson, P.T., eds., Ophiolites in Earth history: Geological Society of London Special Publication 218, p. 481–505.

Harris, R.A., 2006, Rise and fall of the eastern Great Indonesian Arc recorded by the assembly, dispersion and accretion of the Banda Terrane, Timor: Gondwana Research, v. 10, p. 207–231, doi: 10.1016/j.gr .2006.05.010.

Harris, R.A., Sawyer, R.K., and Audley-Charles, M.G., 1998, Collisional mélange development: Geologic associations of active mélange-forming processes with exhumed mélange facies in the western Banda orogen, Indonesia: Tectonics, v. 17, p. 458–479, doi: 10.1029/97TC03083.

Harris, R.A., Kaiser, J., Hurford, A.J., and Carter, A., 2000, Thermal history of Australian passive margin

sequences accreted to Timor during late Neogene arc-continent collision, Indonesia: Journal of Asian Earth Sciences, v. 18, p. 47–69, doi: 10.1016/S1367-9120(99)00036-X.

Huiqi, L., McClay, K.R., and Powell, D., 1992, Physical models of thrust wedges, in McClay, K.R., ed., Thrust Tectonics: New York, Chapman and Hall, p. 71–81.

Kaneko, Y., Maruyama, S., Kadarusman, A., Ota, T., Ishikawa, M., Tsujimori, T., Ishikawa, A., and Okamoto, K., 2007, On-going orogeny in the outer arc of Timor-Tanimbar region, eastern Indonesia, in Santosh, M., and Maruyama, S., eds., Island arcs past and present: Gondwana Research, v. 11, p. 218–233.

Karig, D.E., Barber, A.J., Charlton, T.R., Klemperer, S., and Hussong, D.M., 1987, Nature and distribution of deformation across the Banda Arc-Australian collision zone at Timor: Geological Society of America Bulletin, v. 98, p. 18–32, doi: 10.1130/0016-7606(1987)98<18:NADODA>2.0.CO;2.

Keep, M., Clough, M., Langhi, L., and Moss, S.J., 2002, Neogene tectonic and structural evolution of the Timor Sea region, NW Australia, in Keep, M., and Moss, S.J., eds., Sedimentary basins of Western Australia: Petroleum Exploration Society of Australia Symposium Proceedings, v. 3, p. 341–353.

Klement, K., 1960, Dinoflaggellaten und Hystrichosphaerideen aus dem Malm Suedwestdeutschlands unter besonderer Beruecksichtigung stratigraphisch wichtiger Arten: Palaeontologishe Zeitschrift, v. 34, p. 11.

Kreemer, C., Holt, W.E., and Haines, A.J., 2003, An integrated global model of present-day plate motions and plate boundary deformation: Geophysical Journal International, v. 154, p. 8–34, doi: 10.1046/j.1365-246X.2003.01917.x.

Lambeck, K., and Chappell, J., 2001, Sea level change through the last glacial cycle: Science, v. 292, p. 679–686, doi: 10.1126/science.1059549.

Longley, I.M., Buessenschuett, C., and Clydsdale, L., 2002, The North West Shelf of Australia—A Woodside perspective, in Keep, M. and Moss, S. eds., Sedimentary basins of Western Australia: Petroleum Exploration Society of Australia Symposium Proceedings, v. 3, p. 27–88.

Ludden, J.N., and Dionne, B., 1992, The geochemistry of oceanic crust at the onset of rifting in the Indian Ocean, in Gradstein F.M., and Ludden, J.N., Proceedings of the Ocean Drilling Program, Scientific results, Volume 123: College Station, Texas, Ocean Drilling Program, p. 791–799.

Masson, D.G., Milsom, J., Barber, A.J., Sikumbang, N., and Dwiyanto, B., 1991, Recent tectonics around the island of Timor, eastern Indonesia: Marine and Petroleum Geology, v. 8, p. 35–49, doi: 10.1016/0264-8172(91)90043-Z.

McCaffrey, R., 1988, Active tectonics of the eastern Sunda and Banda Arcs: Journal of Geophysical Research, v. 93, p. 15,163–15,182.

McCaffrey, R., Molnar, P., and Roecker, S.W., 1985, Microearthquake seismicity and fault plane solutions related to arc-continent collision in the eastern Sunda arc, Indonesia: Journal of Geophysical Research, v. 90, p. 4511–4528, doi: 10.1029/JB090iB06p04511.

Merritts, D., and Vincent, K.R., 1989, Geomorphic response of coastal streams to low, intermediate and high rates of uplift, Mendocino triple junction region, northern California: Geological Society of America Bulletin, v. 101, p. 1373–1388, doi: 10.1130/0016-7606(1989)101<1373:GROCST>2.3.CO;2.

Molengraaff, G.A.F., 1912, On recent crustal movements in the Island of Timor and their bearing on the geological history of the East Indian Archipelago: Koninkijke Nederlandse Akademie van Wetenschappen, v. 15, p. 224–235.

Nugroho, H., Harris, R., Amin, W.L., and Maruf, B., 2009, Active plate boundary reorganization in the Banda arc-continent collision: insights from new GPS measurements: Tectonophysics, doi: 10.1016/j.tecto.2009.01.026.

Pearce, J.A., and Cann, J., 1973, Tectonic setting of basic volcanic rocks determined using trace element analyses: Earth and Planetary Science Letters, v. 19, p. 290–300, doi: 10.1016/0012-821X(73)90129-5.

Pirazzoli, P.A., Radtke, U., Hantoro, W.S., Jouannic, C., Hoang, C.T., Causse, C., and Borel-Best, M., 1993, A one million-year-long sequence of marine terraces on Sumba Island, Indonesia: Marine Geology, v. 109, p. 221–236, doi: 10.1016/0025-3227(93)90062-Z.

Ramsay, D.C., and Exon, N.F., 1994, Structure and tectonic history of the northern Exmouth Plateau and Rowley Terrace; outer North West Shelf: AGSO Journal of Australian Geology & Geophysics, v. 15, p. 55–70.

Reed, D.L., Silver, E.A., Prasetyo, H., and Meyer, A.W., 1986, Deformation and sedimentation along a developing terrane suture: Sunda forearc, Indonesia: Geology, v. 14, p. 1000–1003, doi: 10.1130/0091-7613(1986)14<1000:DASAAD>2.0.CO;2.

Roosmawati, N., and Harris, R., 2009, Long-term surface uplift history of the active Banda arc-continent collision: Depth and age analysis of foraminifera from Rote and Savu Islands, Indonesia: Tectonophysics, doi: 10.1016/j.tecto.2009.04.009.

Rutherford, E., Burke, K., and Lytwyn, J., 2001, Tectonic history of Sunda Island, Indonesia, since the Late Cretaceous and its rapid escape into the forearc in the Miocene: Journal of Asian Earth Sciences, v. 19, p. 453–479, doi: 10.1016/S1367-9120(00)00032-8.

Sani, K., Jacobson, M.L., and Sigit, R., 1995, The thin-skinned thrust structures of Timor: Jakarta, Indonesian Petroleum Association 24th Annual Convention, Proceedings, p. 277–293.

Sawyer, R.K., Sani, K., and Brown, S., 1993, The stratigraphy and sedimentology of West Timor, Indonesia: Indonesian Petroleum Association Proceedings, p. 534–574.

Shervais, J.W., 1982, Ti-V plots and the petrogenesis of modern and ophiolitic lavas: Earth and Planetary Science Letters, v. 59, p. 101–118, doi: 10.1016/0012-821X(82)90120-0.

Silver, E.A., Reed, R., McCaffrey, R., and Joyodiwiryo, Y., 1983, Back arc thrusting in the eastern Sunda arc, Indonesia: A consequence of arc-continent collision: Journal of Geophysical Research, v. 88, p. 7429–7448, doi: 10.1029/JB088iB09p07429.

Silver, E.A., Breen, N.A., Prasetyo, H., and Hussong, D.M., 1986, Multibeam study of the Flores back-arc thrust belt, Indonesia: Journal of Geophysical Research, v. 91, p. 3489–3500, doi: 10.1029/JB091iB03p03489.

Snyder, D.B., Prasetyo, H., Blundell, D.J., Pigram, C.J., Barber, A.J., Richardson, A., and Tjokosaproetro, S., 1996, A dual doubly-vergent orogen in the Banda Arc continent-arc collision zone as observed on deep seismic reflection profiles: Tectonics, v. 15, p. 34–53, doi: 10.1029/95TC02352.

Standley, C., and Harris, R., 2009, Banda forearc basement accreted to the NW Australian continental margin: A geochemical, age and structural analysis of the Lolotoi metamorphic complex of East Timor: Tectonophysics, doi: 10.1016/j.tecto.2009.01.034.

Symonds, P.A., Planke, S., Frey, O., and Skogseid, J., 1998, Volcanic evolution of the western Australian continental margin and its implications for basin development: Petroleum Exploration Society of Australia Proceedings, v. 2, p. 33–54.

van der Werff, W., 1995a, Cenozoic evolution of the Savu Basin, Indonesia: Forearc basin response to arc/continent collision: Marine and Petroleum Geology, v. 12, p. 247–262, doi: 10.1016/0264-8172(95)98378-I.

van der Werff, W., 1995b, Structure and morphotectonics of the accretionary prism in the eastern Sunda/western Banda Arc: Journal of Southeast Asian Earth Sciences, v. 11, p. 309–322, doi: 10.1016/0743-9547(94)00038-G.

Van Marle, L.J., van Hinte, J.E., and Nederbragt, A.J., 1987, Plankton percentage of the foraminiferal fauna in seafloor samples from the Australian-Irian Jaya continental margin, eastern Indonesia: Marine Geology, v. 77, p. 151–156, doi: 10.1016/0025-3227(87)90089-2.

van Weering, T.C.E., Kusnida, D., Tjokrosapoetro, S., Lubis, S., and Kridohato, P., 1989, Slumping, sliding and the occurrence of acoustic voids in recent and subrecent sediments of the Savu forearc basin, Indonesia: Netherlands Journal of Sea Research, v. 24, p. 415–430, doi: 10.1016/0077-7579(89)90119-1.

Williams, H.F., Turner, F.J., and Gilbert, C.M., 1982, Petrography, an introduction to the study of rocks in thin section (second edition): San Francisco, W.H. Freeman and Co., 626 p.

Zobell, E., 2007, Origin and tectonic evolution of Gondwana sequence units accreted to the Banda Arc: A structural transect through central East Timor [M.S. thesis]: Provo, Utah, Brigham Young University, 75 p.